



Identification and quantification of lignin monomers and oligomers from reductive catalytic fractionation of pinewood with GC × GC - FID/MS

Journal:	<i>Green Chemistry</i>
Manuscript ID	GC-ART-10-2021-003822.R1
Article Type:	Paper
Date Submitted by the Author:	30-Nov-2021
Complete List of Authors:	Dao Thi, Hang ; Ghent University, Laboratory for Chemical Technology Van Aelst, Korneel; KU Leuven, Centre for Surface Chemistry and Catalysis Van den Bosch, Sander; KU Leuven, Centre for Surface Chemistry and Catalysis Katahira, Rui; National renewable Energy Laboratory, Beckham, Gregg; National Renewable Energy Laboratory, National Bioenergy Center Sels, Bert; KU Leuven, Van Geem, Kevin; Ghent University, Laboratory for Chemical Technology

1 Identification and quantification of lignin monomers and oligomers from 2 reductive catalytic fractionation of pine wood with GC × GC - FID/MS

3 Hang Dao Thi^{†,1}, Korneel Van Aelst^{†,2}, Sander Van den Bosch², Rui Katahira³, Gregg T.
4 Beckham³, Bert F. Sels^{*,2}, Kevin M. Van Geem^{*,1}

5 ¹Laboratory for Chemical Technology, Ghent University, Technologiepark 121, 9052 Ghent, Belgium.

6 ²Center for Sustainable Catalysis and Engineering, KU Leuven, Celestijnenlaan 200F, Leuven 3001, Belgium.

7 ³Renewable Resources and Enabling Sciences Center, National Renewable Energy Laboratory, Golden CO 80401, United
8 States.

9 [†]Both authors contributed equally to this manuscript

10 * Correspondence:

11 E-mail: kevin.vangeem@ugent.be

12 E-mail: bert.sels@kuleuven.be

13 **Key words:** Monophenols, Lignin oligomers, Lignin structure, Fractionation, Reductive Catalytic Fractionation, Biorefinery,
14 GC × GC - FID/MS

15

16 Abstract:

17

18 Thorough lignin characterization is vital to understand the physicochemical properties of lignin
19 and to evaluate lignocellulose biorefinery processes. In this study, an in-depth characterization
20 of lignin oil, obtained from reductive catalytic fractionation (RCF) of pine wood, was
21 performed with quantitative GC × GC - FID analysis and qualitative GC × GC - MS. By
22 utilizing high-temperature resistant column sets in the GC × GC system and by applying a
23 derivatization step, unambiguous detection of lignin monomers, dimers, and trimers is enabled.
24 In addition to confirm the identity of eleven monomers, corresponding to 34 wt% of the RCF
25 lignin oil, thirty-six dimers (16 wt%) and twenty-one trimers (7 wt%) were comprehensively
26 identified by analysis of their mass spectra and quantified by a FID, encompassing the identity
27 of an additional 23 wt% of the RCF lignin oil. The proposed structures reveal the interlinkages
28 present in the dimeric and trimeric oligomers, containing β -5, β -1, β - β , 5-5, and a minor fraction
29 of β -O-4 and 4-O-5 bonds. Furthermore, aliphatic end-units in the dimeric and trimeric
30 molecules were identified, consisting of various substituents at the C4 position, that have been
31 previously observed in the RCF-derived lignin monomers. To reduce complexity for analysis,
32 the RCF oil was separated into six fractions, prior to analysis. The structural motifs (inter-unit
33 linkages and end-units) that are found in the different fractions vary significantly, such that the
34 lignin fractions extracted in more polar solvents contained higher molecular weight fragments
35 and more hydroxyl containing structural motifs. The identified structures of individual dimer
36 and trimer molecules by GC × GC align well with and further complement the recent findings
37 from ¹H-¹³C HSQC NMR spectroscopy, demonstrating complementarity between both 2D
38 techniques to obtain a holistic view on both the molecular structures and the distribution of

39 bonds and end-units in RCF oil. The combination of these two techniques provides a powerful
40 tool for future RCF and other lignin depolymerization research.

41 **Introduction**

42

43 The use of sustainable carbon sources for the production of chemicals and fuels has gained
44 increased attention in the last decades.^{1,2} To this end, lignocellulose holds enormous potential
45 due to its abundance, renewable nature, and composition. It is mainly composed of two
46 polysaccharides, cellulose and hemicellulose, and the aromatic polymer lignin. The latter is
47 formed by radical polymerization of *p*-hydroxyphenyl (H), guaiacyl (G), and syringyl (S) units,
48 among others, in the plant cell wall, forming β -O-4 (β -aryl ether), β -5 (phenylcoumaran), 5-5
49 (dibenzodioxocin), 4-O-5 (diaryl ether), β -1 (spirodienone), and β - β (resinol) inter-unit
50 linkages.^{3,4} Among them, the β -O-4 linkage is most abundant and is relatively labile, making it
51 the target linkage for depolymerization processes to yield aromatic molecules with low
52 molecular weights.⁵⁻⁷

53

54 Many efforts have been made to convert lignin, obtained through various biorefining
55 processes,^{4-6,8-10} into liquid fuels^{11,12} and valuable chemicals (*e.g.* phenol,¹³ polyurethane,¹⁴
56 phenol-formaldehyde (PF) resin,¹⁵ and epoxy resin^{16,17}). One promising biorefining process that
57 emerged notably in recent years is reductive catalytic fractionation (RCF) of lignocellulosic
58 biomass.¹⁸⁻²⁵ During RCF, lignin is extracted with protic solvents (*e.g.* MeOH,¹⁸ alcohol/H₂O²⁶)
59 from lignocellulose, generating phenolic intermediates by selective cleavage of the labile β -O-
60 4 linkages in lignin. Subsequently, these intermediates are stabilized by hydrogenation and
61 hydrogenolysis with a heterogeneous redox catalyst (*e.g.* Pd/C) at elevated temperatures (150 -
62 250 °C) in a reductive environment (*e.g.* hydrogen atmosphere). As a result, the lignin
63 macromolecules are depolymerized, yielding a mixture of phenolic monomers, dimers, and
64 short oligomers.^{24,27-30} Full state of knowledge on RCF can be found in these reviews.^{23,24,30-34}
65 Besides the monomers, there is little molecular understanding of the dimer and oligomer
66 fractions of these RCF oils.³⁰ Given the complex nature of the RCF oil in terms of composition,
67 heterogeneity, and molecular size distribution, solvent-based fractionation can be used to
68 provide relatively homogeneous lignin oil fractions (with regard to molecular weight and
69 structure).^{6,35-37} Consequently, the resulting fractions can provide fruitful information on the
70 molecular weight and its relationship with individual molecular structures (*e.g.* inter-phenolic
71 linkages) and lignin properties such as the hydroxyl content, which are key properties to be
72 considered for the development of the production of new materials and chemicals.^{17,37-39}

73

74 Various analytical techniques have been developed and applied in the analysis of lignin-derived
75 oil samples generated from lignin depolymerization⁴⁰⁻⁴², such as nuclear magnetic resonance
76 (NMR) spectroscopy,⁴³ Fourier-transform infrared resonance (FT-IR) spectroscopy,⁴⁴ gel
77 permeation chromatography (GPC),^{45,46} thermogravimetric analysis (TGA),⁴⁷ and elemental
78 analysis (EA).⁴⁷⁻⁴⁹ However, these analytical tools provide exclusively bulk information of the
79 lignin depolymerization products.⁴⁷⁻⁵³ To separate and individually identify the compounds in
80 (mostly) less/non-volatile oligomeric fractions of (lignin-derived) oil samples, high-pressure
81 liquid chromatography (HPLC) or comprehensive two-dimensional liquid chromatography
82 (LC × LC) combined with high-resolution multi-stage tandem mass spectrometry (HRMSⁿ) is
83 a common method of choice because this technique is not limited by the volatility of the
84 analyte(s). Nonetheless, studies using this approach have focused on monomer identification,
85 through analyzing their mass fragmentation patterns, but not substantially on the oligomers.
86 The comprehensive quantification of oligomers is also inadequate due to the shortage of
87 authentic standard compounds used to support the quantification of the oligomers.⁵⁴⁻⁶⁰ The most
88 popular method to analyze RCF oils is gas chromatography (GC) coupled to mass spectrometry
89 (MS) or a flame ionization detector (FID). However, this approach only allows identification
90 and quantification of the volatile monomeric fractions and a small number of dimers after
91 derivatization.^{18,20,27,46,52,61,62} Furthermore, due to the complex composition of lignin-derived
92 samples, "co-elution" of components with similar physicochemical properties often occurs. As
93 a result, the components can be incorrectly assigned and their quantification thus inaccurate.^{63,64}

94

95 Alternatively, two-dimensional gas chromatography (GC × GC) can be used as it has a higher
96 resolution, larger peak capacity, and higher sensitivity than conventional one-dimensional
97 GC.^{48,53,72,73,63,65-71} Several studies have described the use of GC × GC coupled to a MS/FID
98 detector for qualitative and semi-quantitative analyses of mainly monomers and some dimers
99 in complex bio-oil samples.^{41,56,64,65} Until now, no work has been reported to our knowledge on
100 the detailed molecular characterization of the phenolic oligomers in this complex matrix. The
101 methods that were often applied for quantification consist of: (i) a quantification based on an
102 external quantification method of selected compounds,^{7,67,72} (ii) a quantification in which
103 response factors were calculated based on (modified) effective carbon number factors,^{66,74} or
104 (iii) a relative quantification in which the relative response factors were measured through an
105 internal standard.^{65,72,73,75}

106

107 RCF literature also has focused mainly on the identification and quantification of the phenolic
108 monomers, and only little on the identification of some phenolic dimers in the RCF lignin oil.
109 Structural chemical information of the RCF lignin oligomers that comprise over 40% of the
110 lignin oil has not been detailed, although it is recognized as critical.^{30,52} Recently, a thorough
111 structural study of the pine wood RCF lignin oil was reported that combined solvent
112 fractionation and a variety of classic chromatographic (GC, GC-MS, GPC) and spectroscopic
113 (1D-, 2D-NMR) analyses. This study unambiguously assigned more than 80% of the structural
114 molecular units within the RCF lignin oligomers, including β -5 γ -OH, β -1 γ -OH, β - β 2x γ -OH,
115 β -5 ethyl, β -1 ethyl, β - β THF, and 5-5 inter-unit linkages. However, only monomers and some
116 dimers were characterized individually.²⁷ Here, high-temperature GC \times GC-MS/FID was
117 utilized to comprehensively reveal the individual structural features of the RCF lignin phenolic
118 dimers and trimers from pine wood RCF, including their reliable quantification. Fractionation
119 was used primarily to facilitate the analytical work and product identification. The results
120 provide molecular insight of individual lignin oil components, revealing insight into their
121 formation in the RCF process, and a better understanding of the lignin oil chemical reactivity,
122 which is indispensable to direct further valorization efforts for RCF oil, including but not
123 limited to materials such as polyurethanes^{76,77}, epoxy resins^{17,78}, and others⁷⁹⁻⁸², and chemicals
124 such as antioxidants⁸³ or antimicrobial agents⁸⁴.

125

126

127 **Material and methods**

128

129 *Chemicals*

130 All commercially purchased chemicals in this study were used without further purification.
131 Guaiacol (2-methoxyphenol, 98%), 4-*n*-propylguaiacol (<99%), *N*-methyl-*N*-
132 (trimethylsilyl)trifluoroacetamide (>98.5%), anhydrous pyridine (99.8%), 2-isopropylphenol
133 (>98%), 4-propanolguaiacol (3-(4-hydroxy-3-methoxyphenyl)-1-propanol, >98%), 4-
134 ethylguaiacol (98%), and isoeugenol (2-methoxy-4-propenylphenol, >98%) were purchased
135 from Sigma Aldrich. Acetonitrile (99.9%) and methanol (99.9%) were purchased from
136 ChemLab. 2-Phenoxy-1-phenyl ethanol (**1**), 1-(4-hydroxyphenyl)-2-phenoxy-1,3-propanediol
137 (**2**), and 2-(2,6-dimethoxyphenoxy)-1-(4-hydroxy-3-methoxyphenyl)propane-1,3-diol (**3**),
138 were synthesized as described in the Electronic Supplementary Information (S6, ESI).

139

140 *Sample preparation*

141 Pine wood was soxhlet extracted with an ethanol/toluene mixture (1/2; volume%) for 3h to
142 remove most extractives. The RCF oil is obtained from processing 150 g pre-extracted pine
143 wood for 3 h at 235 °C in a 2 L batch reactor in the presence of 800 mL MeOH, 30 bar H₂, and
144 15 g Pd/C as a catalyst, as described in a previous study.²⁷ The entire RCF lignin oil (F_{oil}) was
145 sequentially fractionated using a binary solvent mixture of heptane (Hept) and ethyl acetate
146 (EtOAc) with increasing polarity. The sequential fractionation steps resulted in 6 lignin oil
147 fractions: F_{H100} (100 vol% Hept/ 0 vol% EtOAc), F_{H80} (80 vol% Hept/ 20 vol% EtOAc), F_{H60}
148 (60 vol% Hept/ 40 vol% EtOAc), F_{H40} (40 vol% Hept/ 60 vol% EtOAc), F_{H20} (20 vol% Hept/
149 80 vol% EtOAc), F_{EA100} (0 vol% Hept/ 100 vol% EtOAc). The detailed preparation of these
150 fractions can be found in our previous study.²⁷

151 Subsequently, an internal standard (IS) was added to a weighed amount of the entire oil F_{oil}
152 sample and the F_{H100}, F_{H80}, F_{H60}, F_{H40}, F_{H20}, F_{EA100} fractions, which were then derivatized before
153 further analysis according to the following procedure: first a small amount of 2-isopropyl
154 phenol (~5 mg), used as an IS, was added into a GC-vial containing a weighted amount of lignin
155 oil (~50 mg). Subsequently, 0.5 mL of anhydrous pyridine, 0.5 mL of *N*-methyl-*N*-
156 (trimethylsilyl)trifluoroacetamide, and 0.5 mL of anhydrous acetonitrile was added. The vial
157 was sealed and put in an oven at 80 °C for 30 minutes. Then, the vial was removed from the
158 oven and cooled to room temperature. Afterward, the sample was analyzed on Thermo
159 Scientific TRACE GC × GC setup (Interscience, Belgium).

160

161 *Analytical method*

162 The GC × GC comprises an Mxt column (60 m × 0.25 mm × 0.25 μm) as the first dimension
163 column connected to a ZB-35HT (2.2 m × 0.18 mm × 0.18 μm) as the second dimension column
164 through a Sil Tite connection. The column set and a dual-state cryogenic modulator (liquid
165 CO₂) are placed in the same oven. The outlet of the second column is connected to an FID/MS
166 detector. For the GC × GC - FID setup, the flow rates of H₂, air, and N₂ (make-up gas) were set
167 at 35, 350, and 35 mL min⁻¹, respectively. The FID temperature was set at 350 °C and the data
168 acquisition rate was 100 Hz. Moreover, a PTV injector was used in these analyses with a
169 programmed temperature injector from 40 °C to 370 °C (hold 25 minutes at 370 °C) to avoid
170 discrimination in the injector. For the GC × GC - MS setup, the data acquisition rate was set at
171 30 spectra s⁻¹ with the scanning range set from 150 to 1100 amu. The GC - MS interface
172 (transfer line) temperature was set at 280 °C and the ion source temperature was set at 300 °C.
173 The MS detector used electron ionization (70 eV). Helium was used as a carrier gas at a constant
174 flow rate (2.1 ml min⁻¹). The modulation period was optimized (10 s) to obtain a maximal

175 resolution in the first dimension without causing wrap-around. The GC system was operated in
176 programmed temperature conditions: 40 °C to 420 °C with a heating rate of 3 °C min⁻¹.

177

178 *Data acquisition and quantification*

179 Thermo Scientific's Chrom-Card data system was used for data acquisition and processing of
180 the FID while Thermo Scientific's XCalibur software was applied for data acquired with the
181 MS. The raw data of GC × GC - FID was exported to a .cdf file, subsequently processed by GC
182 Image (Zoex Corporation, USA) for quantification. The tentative identification of the resulting
183 peaks from GC × GC - FID was achieved by reproducing the analysis using the GC × GC - MS
184 with the identical column combination and an optimized carrier gas flow. Thanks to the stability
185 and linearity of the FID response, the quantification of the identified compounds was, therefore,
186 conducted using the GC × GC - FID chromatogram.

187

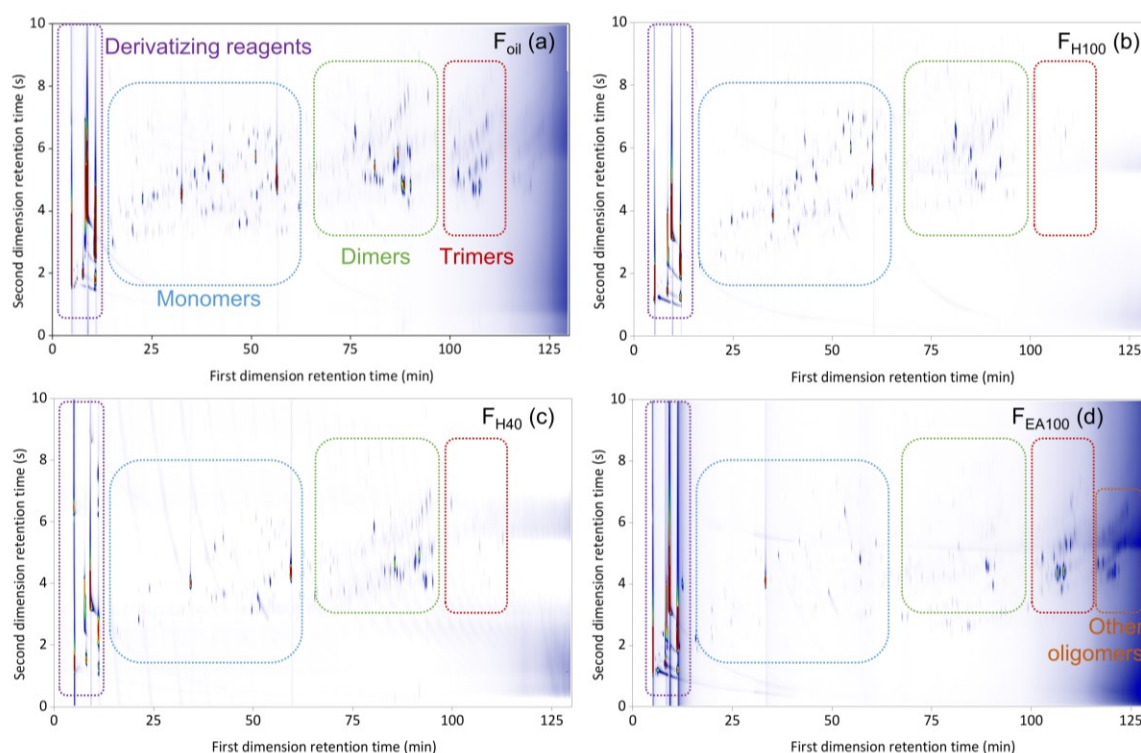
188 **Results and Discussion**

189 *General methodology*

190 GPC results of the RCF lignin oil samples indicated that their composition contains monomers,
191 dimers, and oligomers with varying distribution over the samples and thus varying molecular
192 weights, ranging from 203 to 1,771 g/mol (**Figure S1.1**, see ESI).²⁷ This information reveals
193 that many molecules in these fractions have a high boiling point. Consequently, the GC × GC
194 setup for analyzing RCF lignin samples was equipped with two high-temperature columns with
195 different polarity, allowing chromatographic separation up to 430 °C. Firstly, the use of this GC
196 × GC - FID/MS setup was assessed by measuring an untreated F_{oil} sample. The result of this
197 test revealed that the GC × GC - FID/MS operating at high temperature could elute the
198 monomers, dimers, and a small number of trimers according to three structural regions (**Figure**
199 **S1.2**, see ESI). However, the eluted components often suffered from peak tailing and co-elution,
200 likely due to interaction of hydroxyl groups of the phenolic compounds in the sample either
201 with the glass material of the liner or with the stationary phase of the columns used.⁸⁵ As a
202 consequence, the components present in the sample could be incorrectly assigned and
203 inaccurately quantified. To avoid this issue, the hydroxyl groups of the phenolic compounds
204 were shielded, prior to analyzing on the GC × GC setup, *via* a derivatizing step using *N*-methyl-
205 *N*-(trimethylsilyl)trifluoroacetamide as a reagent. The chromatographic result of the testing F_{oil}
206 sample after derivatization on the GC × GC - FID is illustrated in **Figure 1a**.

207

208 The derivatization step significantly improved the separation of the F_{oil} sample. The phenolic
 209 compounds were eluted in the individual monomeric, dimeric, trimeric, and other oligomeric
 210 regions with well-defined peak shapes. With the key derivatization step in hand, the six
 211 fractions (*i.e.* F_{H100} , F_{H80} , F_{H60} , F_{H40} , F_{H20} , and F_{EA100}) were pretreated accordingly before
 212 analysis. The GC \times GC chromatograms of F_{H80} , F_{H40} , and F_{EA100} are presented in **Figure 1b**,
 213 **Figure 1c**, and **Figure 1d**, respectively, (the chromatogram of F_{H100} , F_{H60} , and F_{H20} fraction can
 214 be found in the ESI, **Figure S1.3 - Figure S1.5**). Thereby, the identification and calculation of
 215 the components present in the seven RCF oil samples will be based on chromatograms of
 216 derivatized samples.



217
 218 **Figure 1.** The GC \times GC color plots of the derivatized entire F_{oil} (a) sample and F_{H80} (b), F_{H40} (c), and F_{EA100} (d)
 219 fractions (Mxt as the first column \times ZB35-HT as the second column).

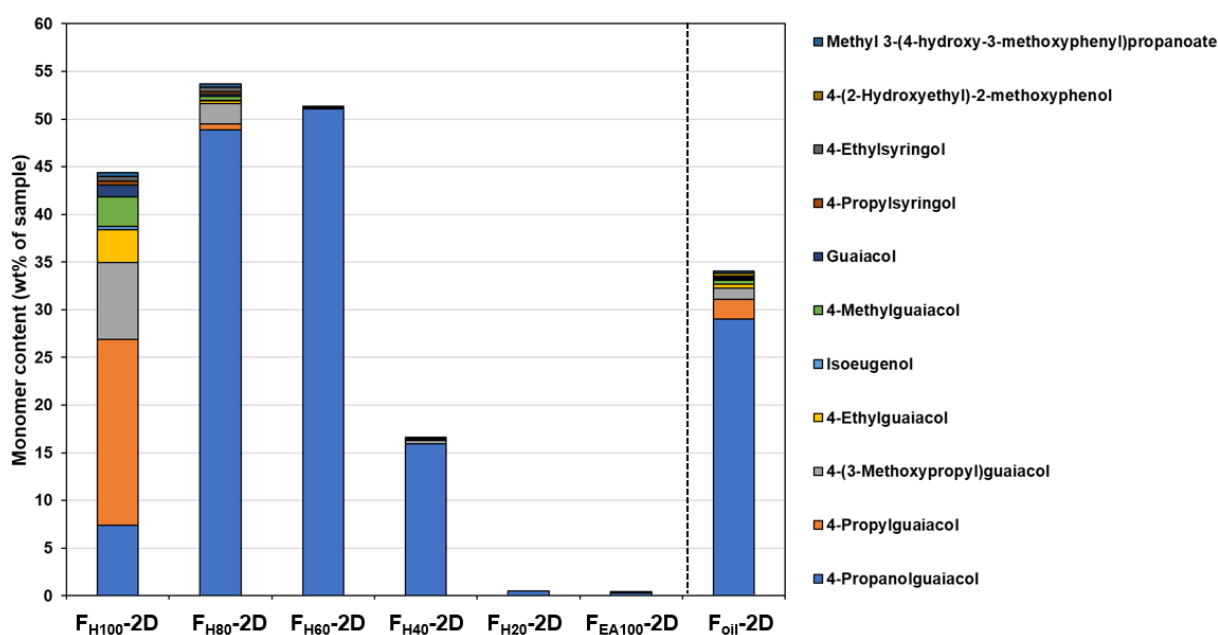
220
 221 *Identification and quantification of lignin-derived phenolic monomers, dimers, and trimers in*
 222 *the RCF lignin oil*

223 The identification of monomers in the RCF lignin oil samples was performed by comparing the
 224 deconvoluted mass spectra obtained from GC \times GC - MS with the NIST library or with retention
 225 indices of authentic monomers. However, this approach could not be applied to the dimers and
 226 trimers due to the limitation of the NIST library and the lack of the authentic dimers and trimers.
 227 The dimeric and trimeric compounds have been assigned based on detailed analysis of their
 228 mass fragmentation patterns (see ESI S3 and ESI S4).

229

230 To accurately quantify the monomers, dimers, and trimers in the RCF oil fractions by GC ×
 231 GC, it strictly requires individual response factors (RFs) between each analyte and the internal
 232 standard. In other words, a library of authentic compounds is required to attain the
 233 corresponding response factors. However, this quantitative approach can solely be applied to
 234 the available monomers, not to oligomers owing to the lack of reference standards. Thus, in this
 235 study, a calibration mixture of monomers and dimers having exact chemical structures (in the
 236 case of monomers) or similar chemical structures (in the case of dimers) of compounds in the
 237 real lignin oil fractions was prepared and measured in the same way as the actual samples (more
 238 information on calibration mixture can be found in **S2** in the ESI). The experimental RFs of
 239 individual components in the calibration mixture were used to determine the RFs of other
 240 components, based on the assumption that the response factor on GC-FID is a function that
 241 depends on the molecular weight of molecules and the number of carbon, hydrogen, oxygen
 242 atoms, and aromatic rings in their structures.^{75,86,87} With these RFs in hand, all the identified
 243 monomers, dimers, and trimers in the seven RCF lignin oil samples were individually
 244 quantified. The monomer quantification using this RF approach on the GC × GC - FID set up
 245 (**Figure 2**) is in line with the results obtained in our previous study,²⁷ for which their RFs have
 246 been determined based on external calibration of the authentic compounds on 1D-GC (The
 247 detailed results of the monomer quantification by GC × GC & 1D-GC can be found in **Table**
 248 **S2.1.**, ESI. Comparison of monomers determined by GC × GC and 1D-GC is presented in
 249 **Figure S2.1**, see ESI).

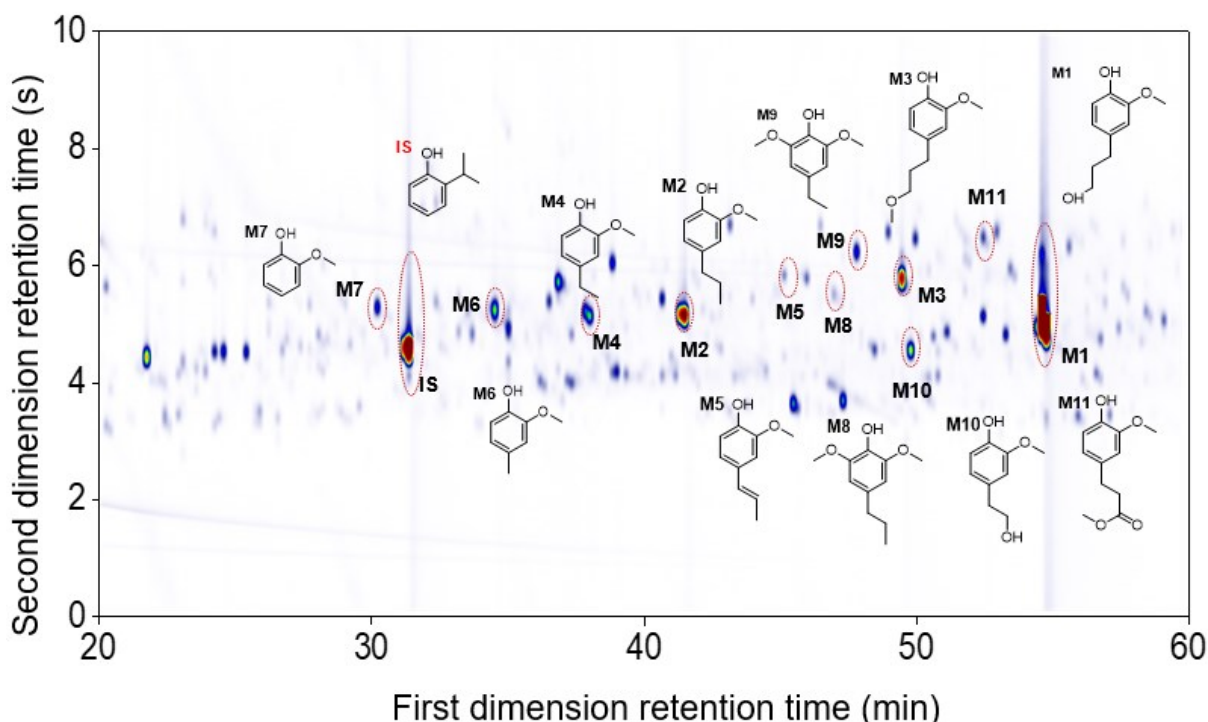
250



251 **Figure 2.** Observable monomers determined by GC x GC - FID. The detailed results of the monomer
252 quantification can be found in **Table S2.1**.

253
254 **Figure 2** shows that the monomer content in the first three fractions (F_{H100} , F_{H80} , and F_{H60}) was
255 enhanced in comparison with the entire F_{oil} sample. Furthermore, in the pure heptane fraction
256 (F_{H100}) the non-polar phenolic monomer (4-propylguaiacol) consists of up to 19.5 wt% of the
257 total monomeric mass fraction. However, 4-propanolguaiacol is the primary monomer in
258 fractions F_{H80} and F_{H60} (48.9 wt% and 51.0 wt%, respectively). Furthermore, the number of
259 monomers decreases significantly in the F_{H40} fraction, whereas negligible amounts were
260 observed in fractions F_{H20} and F_{EA100} . Sequential fractionation by increasing slightly the polarity
261 of solvent thus influences both the distribution and type of monomers in each fraction.

262
263 The use of the high-temperature GC \times GC setup provided a better monomer separation and
264 detection than 1D-GC (more detailed information found in **Table S2.1**, ESI). In particular, the
265 monomers guaiacol (**M7**), 4-propylsyringol (**M8**), 4-ethylsyringol (**M9**), 4-(2-hydroxyethyl)-
266 2-methoxyphenol (**M10**), and methyl 3-(4-hydroxy-3-methoxyphenyl)propanoate (**M11**) were
267 separated and detected on the GC \times GC chromatogram while not clearly visible on the
268 chromatogram of 1D-GC. **Figure 3** illustrates the main monomers found in the F_{oil} sample using
269 the GC \times GC. It should be noted that in all seven RCF lignin oil samples, the G-type monomers
270 were found in a significantly higher content, as expected from using softwood feedstock, but
271 also S-type monomers were observed due to the higher resolution of GC \times GC system, that
272 were not detected on 1D-GC in earlier work.²⁷



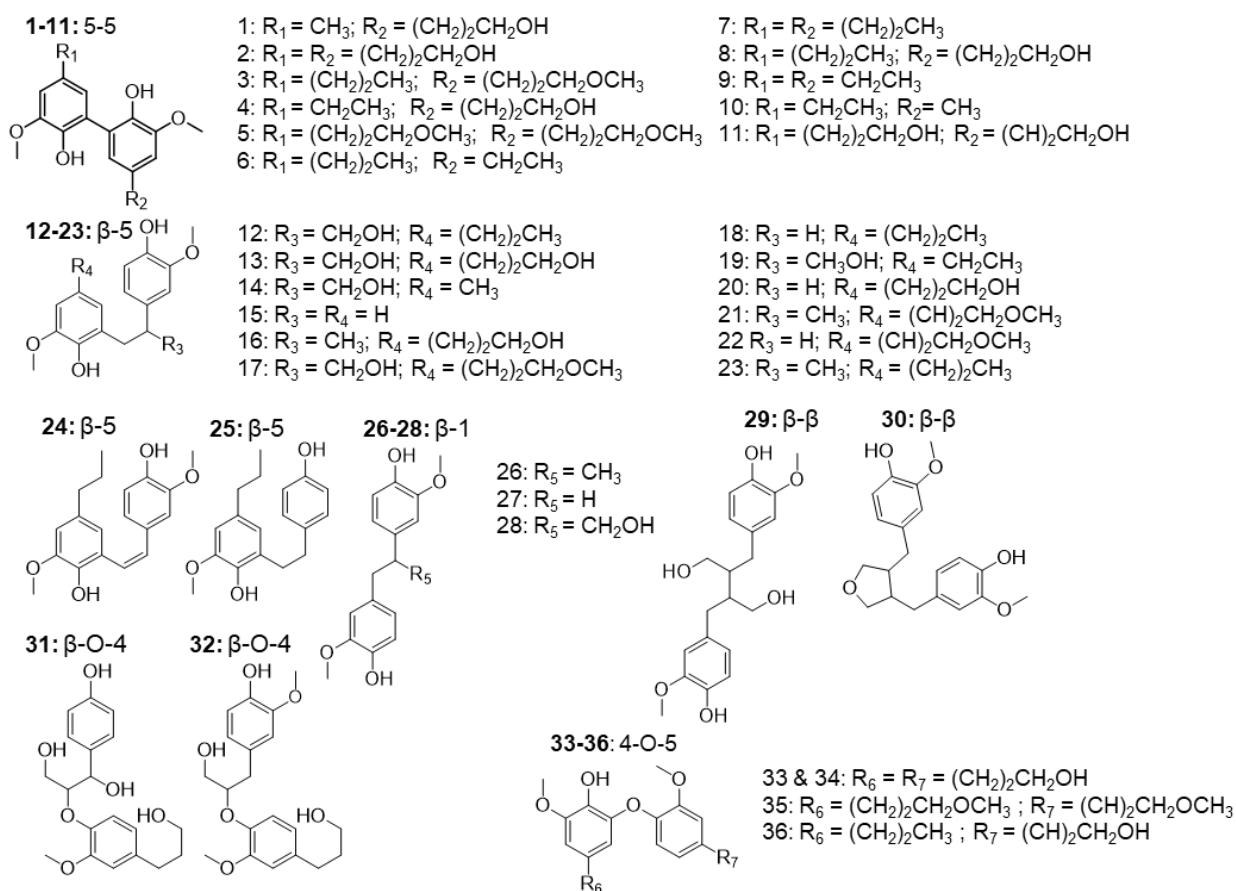
273
274 **Figure 3.** The GC \times GC chromatogram of the monomeric region in the F_{oil} sample.

275
276 In addition to the monomers, analysis of GC \times GC data identified thirty-six phenolic dimers in
277 the RCF lignin fractions, of which only twelve dimers have been previously reported.^{7,18,27,52}
278 Furthermore, twenty-one trimers were also determined for the first time in these fractions (MS
279 information can be found in the ESI, for dimers (**Figure S3.1 - Figure S3.36**) and trimers
280 (**Figure S4.1 - Figure S4.21**)). It is worth noting that not only monomers, dimers, and trimers
281 were detected by using a high peak capacity GC \times GC setup, but also other larger oligomers
282 could be eluted (**Figure 1**). The presence of such oligomers was apparent in the most polar
283 fractions F_{H20} and F_{EA100} (**Figure S1.5** and **Figure 1d**). However, due to the inherent limitation
284 of the GC \times GC - MS and the low concentration of these oligomers, this study only focused on
285 the identification and quantification of the dimers and trimers. **Figure 4** and **Figure 5**
286 summarize the chemical structures

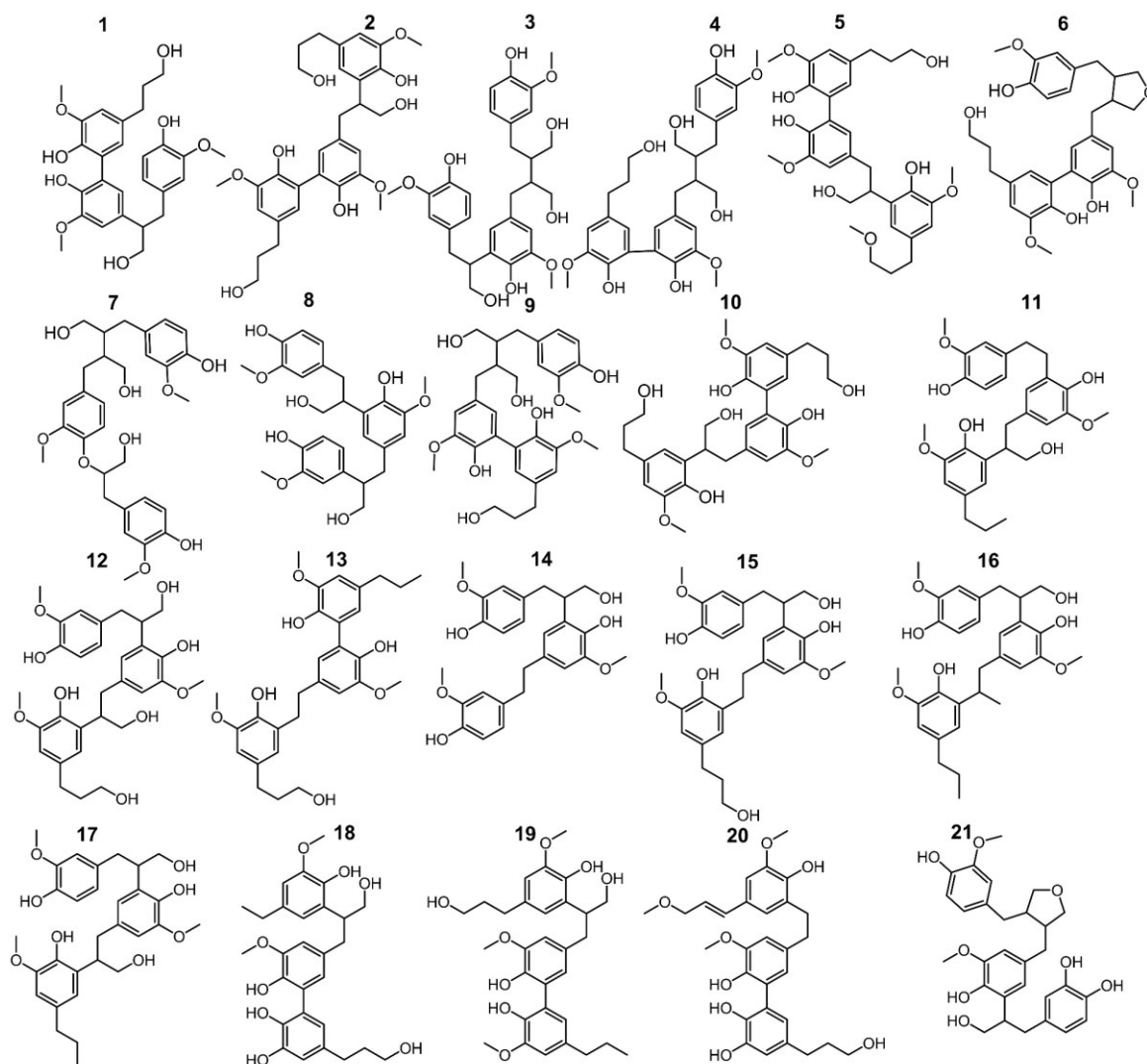
287
288 These dimers and trimers consist of different G units coupled mainly via C-C inter-unit
289 linkages, including β -5 (β -5 γ -OH, β -5 ethyl, and β -5 propyl), β -1 (β -1 γ -OH, β -1 ethyl, and
290 β -1 propyl), β - β (β - β $2\times$ γ -OH and β - β), and 5-5. Furthermore, only a minor number of β -O-4
291 and 4-O-5 inter-linkages were observed in these RCF lignin oil fractions. Most of the inter-unit
292 linkages align well with the bulk information from 1H - ^{13}C HSQC NMR spectroscopy.²⁷
293 However, the 1H - ^{13}C HSQC NMR technique could only assign the inter-unit linkages present

294 of compounds with relatively high concentrations in the entire lignin oil. The inter-unit linkages
 295 with low abundance such as β -5 propyl, β -1 propyl, and 4-O-5 could not be observed properly
 296 by the 2D NMR approach, due to its inherent moderate detection limit. High Temperature-GC
 297 \times GC (HT-GC \times GC) can also identify the aliphatic end-units for the different molecules in the
 298 fractionated RCF lignin oil samples. **Figure 4** and **Figure 5** shows that the aliphatic end-units
 299 in the dimeric and trimeric molecules consist of 4-propanol (4-P- γ -OH), 4-propyl (4-P), 4-ethyl
 300 (4-E), 4-(3-methoxypropyl) (4-P- γ -OMe), 4-methyl (4-M), 4-propenol, and 4-(3-methoxyprop-
 301 1-en-1-yl) as an end-unit. Presence of the two methoxy substituted end-groups indicates some
 302 RCF solvent incorporation in the final products of the RCF biorefinery.

303
 304 The identified dimers and trimers are all composed of similar structural units through the same
 305 inter-unit linkages. This indicates that they have been subject of the same chemistry during RCF
 306 processing; almost all inter-unit ether linkages (*i.e.* β -O-4) are cleaved, whereas the lignin-
 307 original C-C inter-unit linkages remain intact. Furthermore, detailed inspection of the end-units
 308 of the oligomers also reveals strong structural resemblance with those of the monomers.

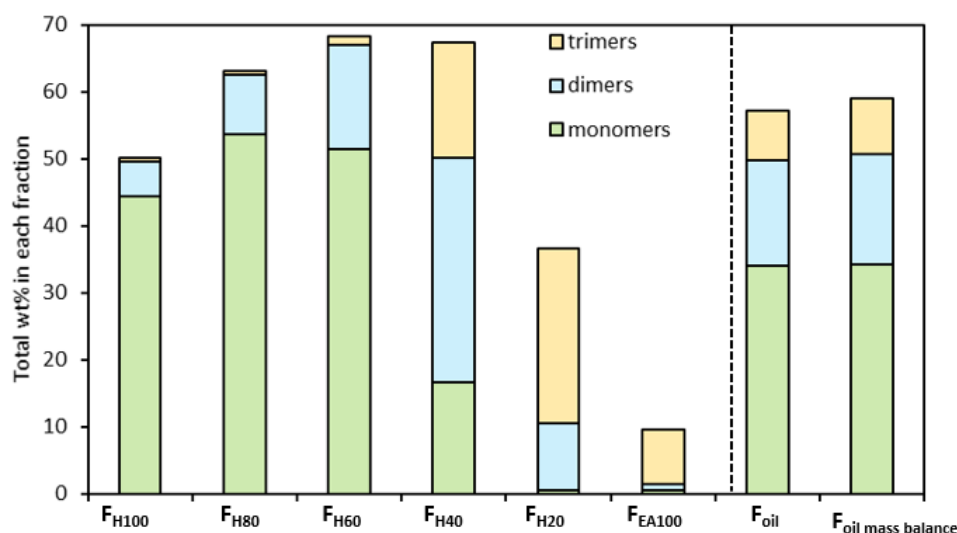


309
 310 **Figure 4.** The structure of observed dimers in the RCF oil samples, derived from the MS spectra using high-
 311 temperature GC \times GC.



312
313 **Figure 5.** The structure of observed trimers in the RCF oil samples, derived from the MS spectra using high-
314 temperature GC × GC.
315

316 Subsequently, the identified dimers and trimers were quantified according to the RF approach
317 explained above. **Figure 6** presents the product distribution and total mass of the monomers,
318 dimers, and trimers in the seven RCF lignin oil fractions (additional information can be found
319 in **Table S2.2**, ESI).



320
 321 **Figure 6.** Distribution and total mass of monomers, dimers, and trimers in the RCF oil samples. Detailed results
 322 can be found in **Table S2.2** and **Table 1**.

323
 324 The quantitative analysis shows that the entire RCF lignin oil (F_{oil}) consists of more monomers
 325 (34.03 wt%, of which 29.01 wt% is 4-propanolguaiacol) than dimers (15.79 wt%) and trimers
 326 (7.26 wt%), respectively. **Figure 6** also shows that only a small number of dimers are found in
 327 the less polar fraction (F_{H100}), whereas the largest amount is found in F_{H40} . Trimers are primarily
 328 observed in 2 fractions (F_{H40} and F_{H20}) and are negligibly present in the less polar fractions
 329 (F_{H100} , F_{H80} , and F_{H60}). Furthermore, almost all monomers, dimers, and trimers were extracted
 330 in the F_{H100} , F_{H80} , F_{H60} , F_{H40} , and F_{H20} fractions, corresponding to 50.11, 62.91, 68.23, 64.63,
 331 and 33.15 wt% of the respective samples. Only 9.64 wt% of the pure ethyl acetate fraction
 332 (F_{EA100}) could be identified. Moreover, the accumulated mass balance of the monomers, dimers,
 333 and trimers over each individual fraction (Fig 5, $F_{oil\ mass\ balance}$) is nearly identical to that of F_{oil} ,
 334 showing the reliability of the analysis. Clearly, the sequential fractionation of the entire RCF
 335 oil (F_{oil}) by using a solvent mixture (Hept/EtOAc) can separate the complicated entire lignin oil
 336 F_{oil} into relatively more homogeneous fractions in terms of molecular weight, in line with the
 337 GPC result in earlier studies,^{88,89} and structural functionality, as revealed here.

338
 339 The detailed quantification of individual dimers (**D**) and trimers (**T**) identified in each lignin oil
 340 fraction is presented in **Table 1**. The result shows that **D2**, **D13**, **D20**, and **D28** are the primary
 341 dimeric molecules found in the entire RCF lignin oil (F_{oil}), corroborating earlier suggestions.²⁷
 342 These dimers contain the same 4-propanol end-group as observed in the monomers, and consist
 343 of 5-5, β -5 γ -OH, β -5 E, and β -1 γ -OH inter-phenolic linkages, respectively. They account for
 344 2.14, 2.81, 1.96, and 2.32, wt% of the total 15.79

345 wt% identified dimers in F_{oil} . Because of the sequential fractionation of the entire F_{oil} , the
346 occurrence of these dimers varied between the fractions. Similarly, **T1**, **T7**, **T4**, and **T2** are the
347 most occurring trimers, corresponding to 0.94, 0.81, 0.80, and 0.72 wt% of the total 7.26 wt%
348 of the identified trimers in the entire lignin oil (F_{oil}). The structural motifs of these trimers
349 consist of 4-propanol end-group, similar to the observed monomers, and contain 5-5 & β -1 γ -
350 OH (**T1**), β -O-4 & β - β 2 \times γ -OH (**T7**), β - β 2 \times γ -OH & 5-5 (**T4**), and β -5 γ -OH & 5-5 (**T2**)
351 inter-unit linkages.
352

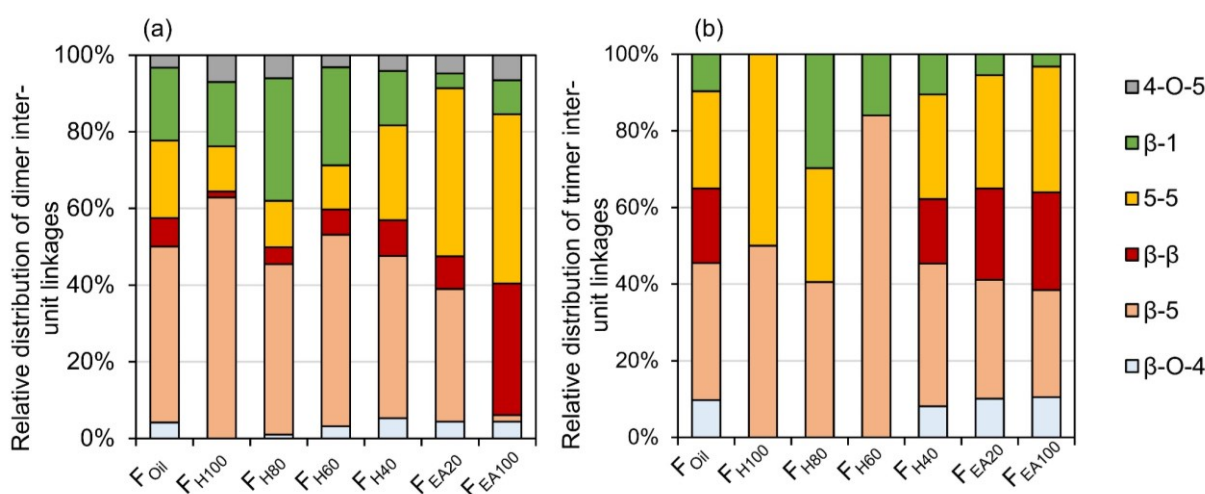
353 **Table 1:** Detailed quantitation of the identified dimers and trimers in 7 RCF lignin oil fractions, expressed in wt%
 354 of the corresponding fraction.

Dimer	F _{oil}	F _{H100}	F _{H80}	F _{H60}	F _{H40}	F _{H20}	F _{EA100}	Trimer	F _{oil}	F _{H100}	F _{H80}	F _{H60}	F _{H40}	F _{H20}	F _{EA100}
D1	0.27	0.00	0.08	0.51	0.51	0.06	0.00	T1	0.94	0.00	0.39	0.00	1.97	2.52	0.60
D2	2.14	0.00	0.04	0.31	6.80	4.09	0.40	T2	0.72	0.00	0.00	0.00	0.60	3.86	1.95
D3	0.08	0.00	0.00	0.00	0.00	0.00	0.00	T3	0.68	0.00	0.00	0.00	0.86	2.60	0.64
D4	0.19	0.00	0.18	0.31	0.25	0.00	0.00	T4	0.80	0.00	0.00	0.00	0.98	5.23	2.57
D5	0.10	0.00	0.04	0.00	0.16	0.03	0.00	T5	0.62	0.00	0.00	0.00	1.24	1.40	0.44
D6	0.00	0.09	0.06	0.00	0.00	0.00	0.00	T6	0.48	0.00	0.00	0.00	1.63	1.02	0.52
D7	0.00	0.20	0.08	0.00	0.00	0.00	0.00	T7	0.81	0.00	0.00	0.00	1.04	2.16	0.77
D8	0.31	0.00	0.19	0.60	0.33	0.00	0.00	T8	0.21	0.00	0.00	0.00	0.33	0.00	0.00
D9	0.00	0.13	0.13	0.00	0.00	0.00	0.00	T9	0.17	0.00	0.00	0.00	0.85	0.38	0.00
D10	0.00	0.07	0.06	0.00	0.00	0.00	0.00	T10	0.17	0.00	0.00	0.00	0.38	0.16	0.00
D11	0.09	0.00	0.00	0.09	0.24	0.15	0.02	T11	0.19	0.00	0.00	0.00	0.00	0.28	0.00
D12	0.25	0.00	0.32	0.48	0.15	0.00	0.00	T12	0.36	0.00	0.00	0.00	0.52	1.05	0.36
D13	2.81	0.00	0.12	1.28	9.06	3.18	0.00	T13	0.10	0.46	0.00	0.00	0.00	0.00	0.00
D14	0.06	0.11	0.25	0.00	0.00	0.00	0.00	T14	0.32	0.00	0.14	0.38	1.13	0.27	0.00
D15	0.00	0.00	0.03	0.00	0.00	0.00	0.00	T15	0.41	0.00	0.00	0.82	0.63	0.48	0.18
D16	0.01	0.00	0.00	0.00	0.00	0.00	0.00	T16	0.11	0.00	0.00	0.00	0.00	0.00	0.00
D17	0.54	0.00	0.10	0.77	1.04	0.10	0.02	T17	0.15	0.00	0.00	0.00	0.00	0.00	0.00
D18	0.55	2.97	1.26	0.00	0.00	0.00	0.00	T18	0.00	0.00	0.00	0.00	0.30	0.20	0.00
D19	0.07	0.00	0.08	0.13	0.05	0.00	0.00	T19	0.00	0.00	0.00	0.00	0.39	0.00	0.00
D20	1.96	0.12	1.01	3.57	2.79	0.14	0.00	T20	0.00	0.00	0.00	0.00	0.55	0.39	0.00
D21	0.08	0.00	0.05	0.07	0.09	0.00	0.00	T21	0.00	0.00	0.00	0.00	1.15	0.80	0.23
D22	0.23	0.00	0.10	0.30	0.33	0.00	0.00	Total	7.26	0.46	0.54	1.20	14.55	22.78	8.26
D23	0.04	0.15	0.06	0.00	0.00	0.00	0.00								
D24	0.21	0.00	0.15	0.30	0.25	0.00	0.00								
D25	0.00	0.00	0.14	0.00	0.00	0.00	0.00								
D26	0.17	0.30	0.54	0.18	0.00	0.00	0.00								
D27	0.51	0.50	1.60	0.61	0.06	0.00	0.00								
D28	2.32	0.11	0.67	3.22	4.68	0.38	0.08								
D29	0.85	0.00	0.06	0.56	2.85	0.84	0.33								
D30	0.33	0.08	0.33	0.47	0.28	0.00	0.00								
D31	0.10	0.00	0.00	0.00	0.24	0.14	0.00								
D32	0.56	0.00	0.09	0.50	1.52	0.29	0.04								
D33	0.52	0.00	0.07	0.50	1.38	0.47	0.06								
D34	0.46	0.04	0.44	0.94	0.39	0.00	0.00								
D35	0.00	0.22	0.18	0.00	0.00	0.00	0.00								
D36	0.00	0.16	0.15	0.00	0.00	0.00	0.00								
Total	15.79	5.28	8.68	15.68	33.47	9.87	0.95								

355

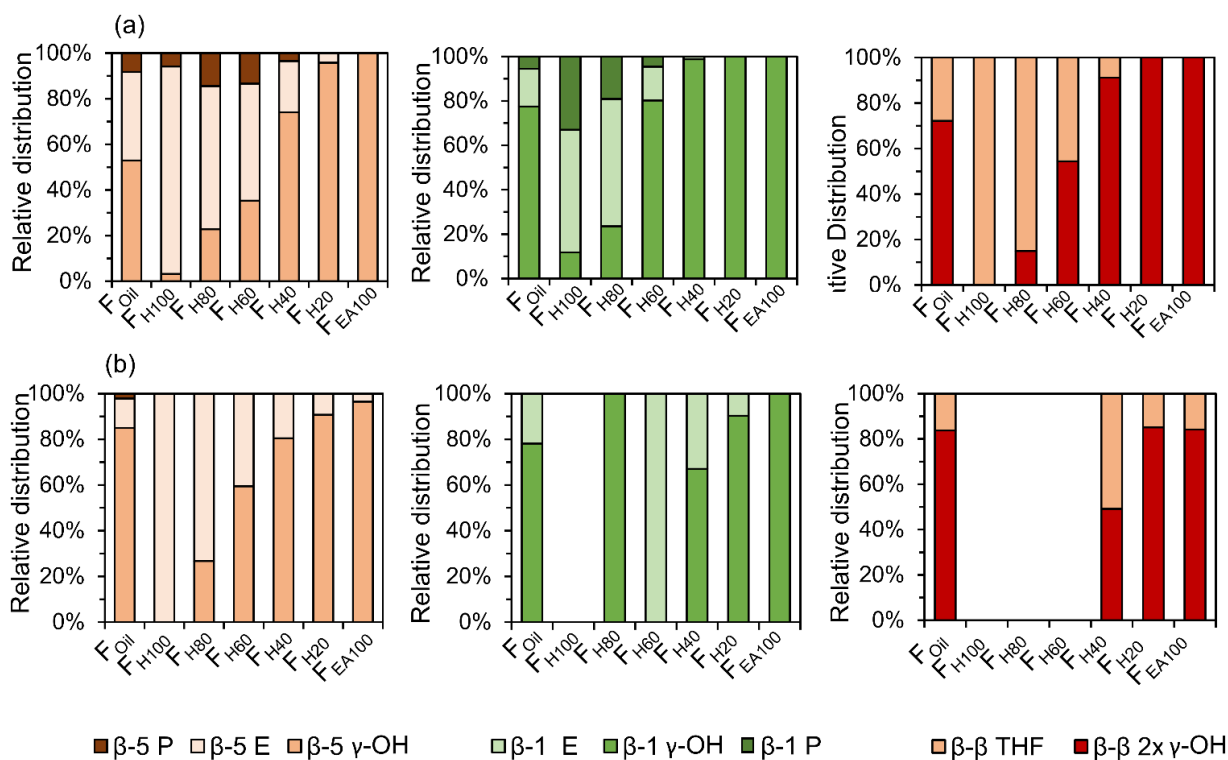
356 *Inter-unit linkages and end-groups of dimers and trimers in the pine wood RCF lignin oil*

357 The quantitative GC × GC results of the dimers and trimers show that the structural motifs of
 358 these molecules consist of inter-unit linkages including β -5, β -1, β - β , 5-5, β -O-4, 4-O-5 and
 359 aliphatic end-units including 4-P- γ -OH, 4-P, 4-E, 4-P- γ -OMe, 4-M, 4-propenol, and 4-(3-
 360 methoxyprop-1-en-1-yl). A fraction-dependent distribution between these structural motifs and
 361 the increasing polarity of the extraction solvent can be observed in **Figure 7**. These relative
 362 distributions are calculated based on the individual mole% of the dimers and trimers relative to
 363 the total mole% of dimers and trimers. Furthermore, the individual distribution of β -5, β -1, and
 364 β - β inter-unit linkages in the RCF lignin oil, based on the dimer and trimer molecular
 365 identification, is also depicted in **Figure 8**.



366
 367 **Figure 7.** Relative distribution of inter-unit linkages based on wt% of the corresponding dimers (a) and trimers
 368 (b) in the RCF lignin oil.

369



370 β -5 P β -5 E β -5 γ -OH β -1 E β -1 γ -OH β -1 P β - β THF β - β 2x γ -OH
 371 **Figure 8.** Individual distribution of β -5, β -1, and β - β inter-unit linkages of dimers (a) and trimers (b) in the RCF
 372 lignin oil.

373
 374 The first inter-unit linkage discussed herein is the β -5 inter-unit linkage, which is composed of
 375 β -5 γ -OH (e.g. **D13**), β -5 ethyl (e.g. **D16**), and β -5 propyl (e.g. **D16**) analogs, originating from
 376 the native β -5 phenylcoumaran structure. Over 45 wt% of the identified dimers in the entire
 377 RCF oil (F_{oil}) contain a β -5 inter-unit linkage and over 59 wt% of the identified trimers in F_{oil}
 378 contain at least one β -5 inter-unit linkage in the structure. Given always two inter-unit linkages
 379 are present in trimers, approximately 34% of all inter-unit linkages in trimers contains the β -5
 380 structure (**Figure 7**). Among these β -5 inter-unit linkages, β -5 γ -OH is most abundant in both
 381 dimers and trimers (relative amount of 51% and 84%, respectively; **Figure 8**). Furthermore, the
 382 distribution of β -5 analogs of dimers and trimers varied between fractions. For example, β -5
 383 dimers are predominant (63%) in the fraction F_{H100} (**Figure 7a**), with mostly the β -5 E linkage
 384 (**Figure 8a**). Only a small amount of these β -5 units (1.7%) is present in the most polar fraction
 385 F_{EA100}, with sole contributor β -5 γ -OH. Overall, the high β -5 γ -OH occurrence increases at the
 386 expense of β -5 E (**Figure 8**); this accords with the solvent polarity.

387
 388 The β -1 motifs, consisting of β -1 γ -OH (e.g. **D28**), β -1 ethyl (e.g. **D27**), and β -1 propyl (e.g.
 389 **D26**) analogs, are a second group of inter-unit linkages present in the RCF lignin oil.
 390 Approximately 19 wt% of the identified dimers in F_{oil} and over 20 wt% of the identified trimers

391 in F_{oil} have one β -1 inter-unit linkage, indicating that approximately 10% of the inter-unit
392 linkages in the identified trimers holds a β -1 structure (**Figure 7**). The β -1 γ -OH analog
393 predominates in both dimers and trimers, showing a relative occurrence of 77% and 78%,
394 respectively (**Figure 8**). Presence of β -1 γ -OH increases with solvent polarity, similarly as
395 observed for β -5 (**Figure 8**). Moreover, presence of β -1 decreases with solvent polarity (**Figure**
396 **7**). These observations of less β -1 in the trimers, compared to the dimers, and less β -1 in the
397 more polar (higher molecular weight containing) fractions, is likely the consequence of the
398 native-lignin structure. That is, in the β -1 spirodienone structure, one of the two phenolics of
399 the β -1 linkage is a quinone methide, remaining unsubstituted on its phenolic and 5-position.³
400 Thus, only a linkage to a third phenolic group can be made through the second phenolic moiety.
401 Given the high chance of this being a β -O-4 linkage in accordance with lignin formation
402 mechanisms⁹⁰, relatively more β -1 inter-unit linkages are present in a dimer form, as observed
403 in **Figure 7**.

404
405 The β - β linkages are the third group of inter-unit linkages discussed herein. They originate from
406 the native β - β resinol structure, and after subjecting to the RCF process this resinol structure is
407 converted to β - β $2\times$ γ -OH (*e.g.* **D29**) and β - β THF (*e.g.* **D30**). Around 7 wt% of the identified
408 dimers and over 37 wt% of the trimers contain a β - β structure in F_{oil} (**Figure 7**), indicating that
409 approximately 20% of the inter-unit linkages in trimers has a β - β structure (**Figure 7**). The β - β
410 $2\times$ γ -OH linkage in both dimers and trimers is more abundant than β - β THF (**Figure 8**). **Figure**
411 **7** and **8** also shows that the relative number of β - β linkages and β - β $2\times$ γ -OH's presence in both
412 dimers and trimers increases with increasing polarity of the extraction solvent, while β - β THF
413 is mainly present in the less polar fractions (*e.g.* dimer fraction F_{H100} and F_{H80}) (**Figure 8a**).

414
415 It can be concluded that a significant amount of the γ -OH functional group in the inter-unit
416 linkages of β -5, β -1, and β - β units in both dimers and trimers is observed in the more polar,
417 higher molecular weight fractions (*e.g.* F_{H40} , F_{H20} , and F_{EA100}), compared to the inter-unit
418 linkages without γ -OH group. Thus, the oligomers containing the polar inter-unit linkages will
419 be mainly extracted in more polar solvents, and they are, conversely, less soluble in the
420 non/less-polar solvents. This observation supports the bulk results obtained from ^1H - ^{13}C HSQC
421 NMR spectroscopy.²⁷

422
423 The fourth group is the biphenyl (5-5) inter-unit linkage, originating from the dibenzodioxocin
424 inter-unit linkages in native lignin. Approximately 20 wt% of the detected dimers and 51 wt%

425 of the detected trimers in F_{oil} contain this 5-5 linkage, and thus 25% of the inter-unit linkages
426 in the identified trimers have a 5-5 structure. Dimers containing 5-5 are present in considerably
427 higher amounts in the more polar (higher molecular weight) fractions (**Figure 7a**). An
428 increasing trend of 5-5 containing trimers in the F_{H40} , F_{H20} , and F_{EA100} fractions with the higher
429 polarity is also apparent in **Figure 7b**. However, **Figure 7b** shows that the 5-5 trimers account
430 for up to 50% of inter-unit linkages in the non-polar fraction F_{H100} . The reason for this is that
431 only one trimer is detected in F_{H100} , of which one of the inter-unit linkages has the 5-5 structure.
432 This is because this non-polar extraction solvent impedes the solubility and extraction of
433 trimers.

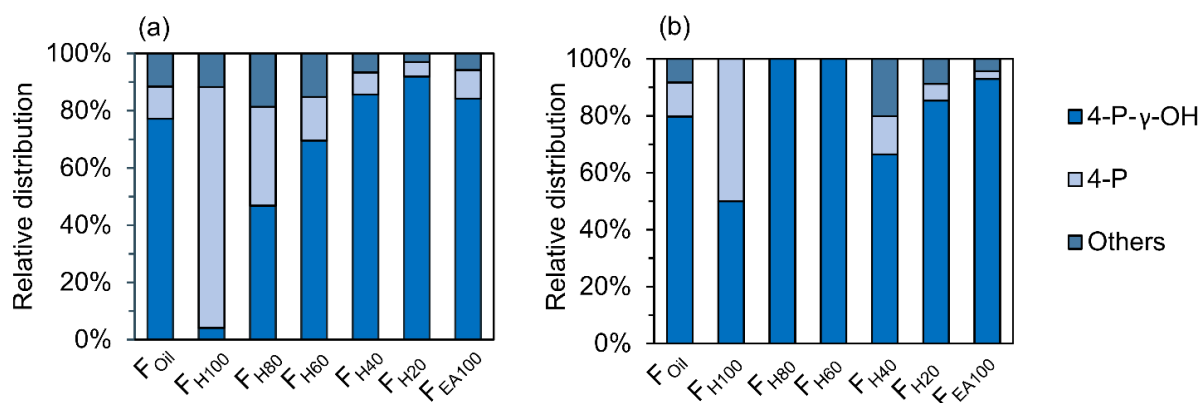
434
435 Small amounts of β -O-4 inter-unit linkages that remained after RCF processing are also
436 detected in dimers and trimers of the entire oil (F_{oil}) (**Figure 7**). Strikingly, the majority of
437 detected β -O-4 structure underwent a α -dehydroxylation, yielding a reduced form of the native
438 β -O-4 structure (e.g. **Figure 5**, T7). This α -dehydroxylation reaction product has been
439 previously observed in minor amounts when using Pd/C catalysis on β -O-4 model compounds.
440 It was suggested to be a side product of the concerted catalytic β -O-4 cleavage.⁹¹ The
441 occurrence of β -O-4 linkages increases in the high molecular weight fractions of dimers and
442 trimers. Given their low occurrence - relative to the other inter-unit linkages - most of the β -O-
443 4 linkages were effectively cleaved during the RCF process. Moreover, most of the non-cleaved
444 β -O-4 structures has undergone a reductive reaction, yielding a reduced form of β -O-4.

445
446 Lastly, in 3 wt% of the dimers (in the entire oil, F_{oil}), a 4-O-5 inter-unit linkage was found,
447 while absent in the structure of the trimers. It should be noted that these 4-O-5-linked structures
448 have never been detected by NMR techniques in the previous studies on RCF lignin. This is
449 possibly due to the low concentration level of these units in the lignin oil. This example
450 illustrates the high sensitivity of the GC \times GC-FID/MS method as compared to that of the 2D
451 NMR technique.^{27,92,93}

452
453 Next to the inter-unit linkages, end-units resulting from β -O-4 cleavage and the reductive
454 chemistry during RCF processing are another important structural motif. These groups consist
455 of 4-P- γ -OH, 4-P, 4-E, 4-P- γ -OMe, 4-M, 4-propenol, and 4-(3-methoxyprop-1-en-1-yl) units.
456 Among them, the 4-P- γ -OH and 4-P end-units are found at high amounts in the various RCF
457 lignin oil fractions (**Figure 9**). The other end-units, including 4-E, 4-P- γ -OMe, 4-M, 4-

458 propanol, and 4-(3-methoxyprop-1-en-1-yl)) are detected with relatively low abundance in the
 459 dimer and trimer structures, and therefore they are combined as “Others” in **Figure 9**.

460
 461 Around 80% of 4-P- γ -OH end-unit is found in both dimers and trimers, whilst only
 462 approximately 10% of the 4-P unit is observed in both dimers and trimers of the F_{oil} fraction
 463 (**Figure 9**). This is the consequence of the reduction chemistry with Pd catalysis, showing (as
 464 in the monomer fraction) large quantities of propanol end groups due to its low oxophilic
 465 character.¹⁰ It is also recognized that the presence of the P- γ -OH end-unit in dimers increases
 466 steadily with the increasing polarity of the fractions (**Figure 9a**). A similar observation can be
 467 made for the trimers in $F_{H40-EA100}$. **Figure 9** also indicates that the 4-P end-unit is most prevalent
 468 in the non-polar fraction (F_{H100}) of both dimers and trimers. Obviously, this is the result of the
 469 favorable extraction of less polar 4-P substitution in pure heptane, while the more polar P- γ -
 470 OH end-unit is preferably extracted in the polar solvents.

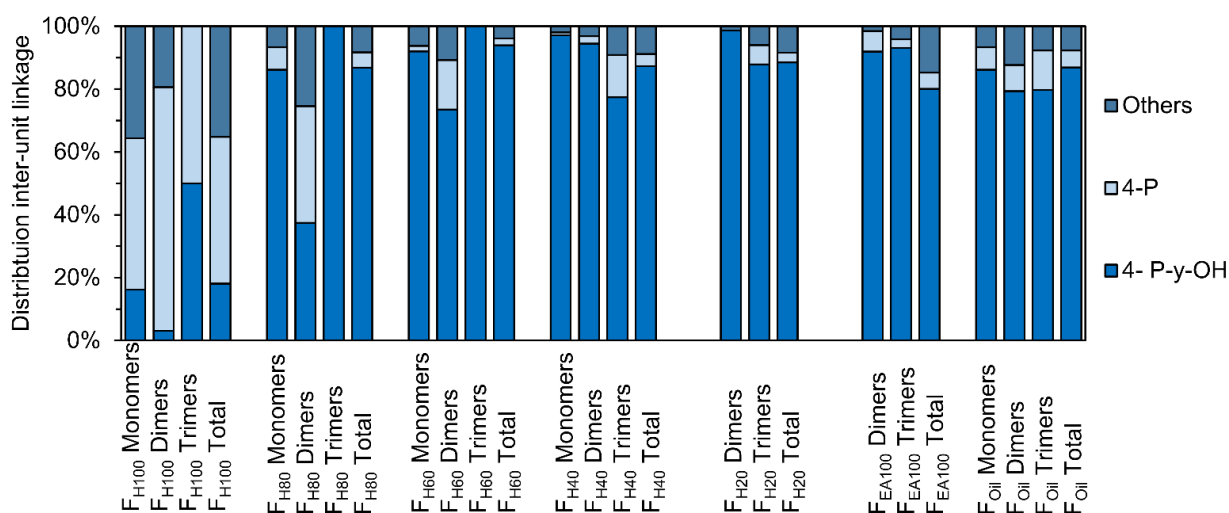


471
 472 **Figure 9.** Relative distribution of end-unit groups in dimers (a) and trimers (b) of the RCF lignin oil.

473 $GC \times GC$ - NMR correlation

474 Similar solvent fractionation was used (for sample preparation) in an earlier study presenting
 475 structure elucidation of RCF lignin oil using 1H - ^{13}C HSQC NMR spectroscopy. The advantage
 476 of this particular method is that a specific end-unit or inter-unit linkage only has a limited
 477 amount of C-H correlation signals, which are independent of the individual molecular structure.
 478 For example, a dimer containing a β -5 ethyl (β -5 E) inter-unit linkage will have the same β -5 E
 479 C-H correlation pairs as a trimer also containing β -5 E. Hence, the total relative distribution of
 480 a specific inter-unit linkage or end-unit can be quantified for the entire RCF lignin oil. A general
 481 disadvantage of this spectroscopic method is that only bulk information of these molecular
 482 structures is obtained. Accordingly, it is challenging to investigate differences in the distribution
 483 of specific structures in specific classes (*viz.* monomers, dimers, trimers, etc.). Besides, the
 484 technique has sensitivity limits, as known for NMR spectroscopy. The high-resolution $GC \times$

485 GC method developed herein solves this latter issue, providing more detailed structural
 486 information, also of the minor compounds in the RCF lignin oil. To investigate if large
 487 differences in distribution can be observed between (in mole%; monomers, dimers, and trimers between
 488 these classes and the entire lignin oil, the structural relative distributions obtained by GC × GC)
 489 are compared with the relative distributions obtained by ^1H - ^{13}C HSQC NMR spectroscopy by
 490 analysis of the entire sample (in mole%, total).



491
 492 **Figure 10.** Comparison of distribution of end-units, divided in 4-P- γ -OH, 4-P, and “Others” in the different RCF
 493 lignin fractions. The monomer, dimer, and trimer distribution is obtained by GC × GC. The distribution of each
 494 total fraction is obtained by ^1H - ^{13}C HSQC NMR spectroscopy.⁹

495
 496 As shown in **Figure 10**, the effect of the extraction solvent has a clear influence on the
 497 distribution of end-units, as discussed earlier. For almost all fractions, the relative occurrence
 498 of a specific end-unit obtained by the ^1H - ^{13}C HSQC NMR spectroscopy lies between that of the
 499 specific fractions (*i.e.* monomer, dimer, and trimer) of a certain sample, validating the GC ×
 500 GC analysis. Thus, in addition to the insight in chemical structure (from MS), the accumulated
 501 quantified information from GC × GC - FID accords with the bulk information delivered by
 502 ^1H - ^{13}C HSQC NMR spectroscopy.

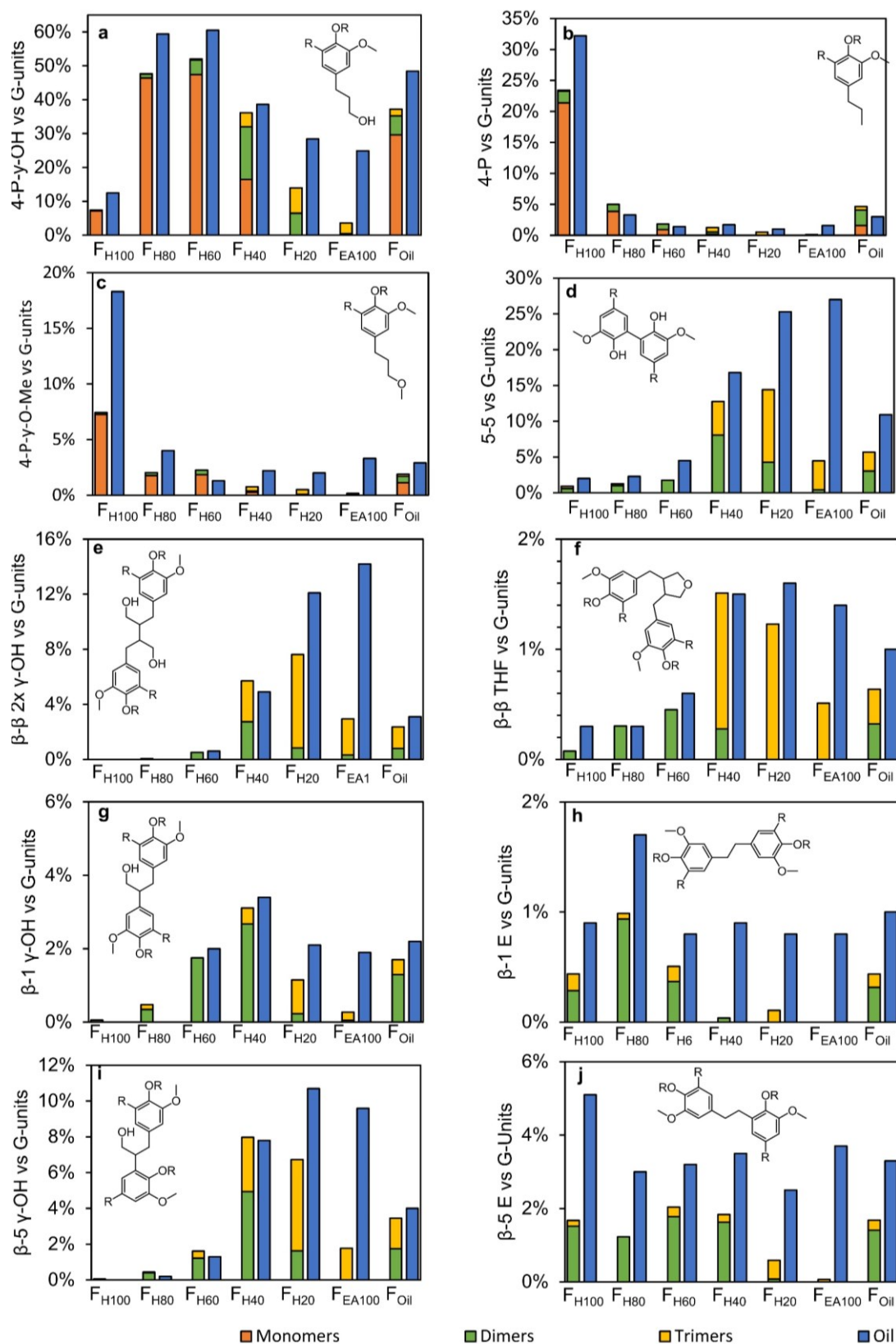
503
 504 Just as for the end-units, the distribution differences for the various inter-unit linkages are
 505 shown in **Figure S5 (Figure S5.1 - Figure S5.3, see ESI)** and similar trends can be observed.
 506 That is, the occurrence of the typical RCF β -5, β -1, and β - β structures found by GC × GC and
 507 NMR analysis are comparable for fraction F_{oil}. One noticeable exception is the very low β -5 E
 508 substitution in the entire lignin oil’s trimer fraction, compared to the two times higher β -5 E
 509 substitution observed in the entire oil. The reason for this might lie either in a reactivity

510 difference during the RCF process (*i.e.* lower reactivity to form β -5 E in trimers) or in the GC
511 \times GC detection. Indeed, while an even amount of dimers bearing the β -5 E or β -5 γ -OH group
512 are identified, four times more β -5 γ -OH structures are identified in the trimers as compared to
513 the β -5 E. Since not all trimer signals were identified and quantified, the possible lower catalytic
514 selectivity to the β -5 E linkage might thus simply be enhanced by the low number of identified
515 β -5 E containing signals.

516
517 Besides comparing product distribution of the RCF process, as ascertained by GC \times GC analysis
518 and ^1H - ^{13}C HSQC NMR spectroscopic analysis, the overall yield of the specific molecular
519 structures obtained by GC \times GC analysis can also be constructed and compared with the ^1H -
520 ^{13}C HSQC NMR spectroscopic results. This furthers the insight into the distribution of a certain
521 molecular structure in the monomers, dimers, and trimers relative to the entire oil. As the ^1H -
522 ^{13}C HSQC NMR spectroscopic results are expressed in relative percentage per guaiacyl unit,
523 the GC \times GC results were recalculated according to formulas in **Note S5.4** (see ESI).

524
525 Before going into detail, a few important remarks on the interpretation of these results must be
526 made. First, the results of two powerful analytical techniques are combined, each with their
527 advantages and disadvantages. The obvious advantage of GC \times GC is the identification of
528 individual molecular structures. However, compounds which are only present in a very small
529 amount are hard and laborious to detect, identify and quantify. Consequently not all molecules,
530 containing a specific molecular structure are taken into account in this calculation, negatively
531 effecting molecular structures with a low abundance; *viz.* there are still unassigned trimers.
532 Besides, by recalculating the GC \times GC results (in wt% or mole%) to the ‘relative abundancy
533 *vs.* G-units’, the assumption has been made that 100% of each sample’s mass is lignin. Whereas
534 this is evidently more correct for the more polar samples (because of the almost closure of some
535 balances), this is less correct for the less polar samples, likely the consequence of the presence
536 of some non-polar extractives. One major disadvantage of ^1H - ^{13}C HSQC NMR spectroscopy is
537 that its quantification is only on a relative scale (*vs.* the aromatic part) and that the spectroscopic
538 related issues (such as the $J_{\text{C-H}}$ dependency or relaxation effects) might play a large role in
539 comparing these relative quantitated structures with the absolute quantitated structures by GC
540 \times GC. Despite these barriers, the results of these product distributions still contain various
541 relevant trends, as shown in **Figure 11**.

542



543

544 **Figure 11.** Distribution of the end-units and inter-unit linkages found in the monomers, dimers and trimers in the
 545 different fractions and compared to their amounts found in the entire sample. The monomer, dimer and trimer
 546 distribution is quantified according to **Note S5.4** (see **ESI**). The results of the oil are obtained by ^1H - ^{13}C HSQC
 547 NMR spectroscopy.⁹

548

549 Firstly, it is obvious from **Figure 11a-c** that the monomers account for by far the largest amount
550 of end-units. Yet, in certain fractions from intermediate polarity (*viz.* F_{H40} and F_{H20}), also the
551 dimers and trimers make up for a large part of the end-units (**Figure 11a**). Overall, in the results
552 obtained by ¹H-¹³C HSQC NMR spectroscopy, almost in all cases more end-units have been
553 observed in the fractions. In F_{H100}, F_{H80}, and F_{H60}, this can likely be ascribed to the reasons noted
554 above, *viz.* presence of non-lignin molecules, analytical complexity, since only a minor amount
555 of RCF lignin trimers are present in these fractions, excluding the possibility of higher
556 molecular weight structures - which is also in correspondence with the GPC result (**Figure S1**).
557 However, in F_{H40}, F_{H20}, and F_{EA100}, the higher amount of end-units observed by ¹H-¹³C HSQC
558 NMR spectroscopy is likely the consequence of the undetected dimers and trimers, and the
559 presence of higher molecular weight structures, such as RCF lignin-derived tetramers,
560 pentamers, etc., which cannot be analyzed by the GC × GC technique due to too high
561 evaporation temperatures of the products.

562

563 Secondly, between 40-80% of a specific inter-unit linkage quantified in ¹H-¹³C HSQC NMR
564 spectroscopy can be accounted for by the observed dimers and trimers (**Figure 11d-j**),
565 indicating that a considerable amount of the RCF lignin inter-unit linkages are present in the
566 observed RCF dimers and trimers. More detailed interpreting of the distribution of specific
567 inter-unit linkages has to be done with caution, due to the above described barriers arising from
568 the construction of these figures. This is likely the consequence of the low number of identified
569 trimers bearing these inter-unit linkages.

570

571

572 3. Conclusion

573 This study shows both the comprehensive identification and quantification of the dimeric and
574 trimeric phenolic oligomers in the RCF lignin oil of pine wood. The successful combination of
575 the high-temperature GC × GC - FID and GC × GC - MS, besides fractionation of lignin oil
576 using varying solvent polarity, allows to unambiguously assign molecular structures of thirty-
577 six dimers and twenty-one trimers in the RCF lignin oil samples. Derivatization of these lignin
578 samples was critical to prevent peak-tailing and co-eluting effects. The detailed structural
579 information in terms of inter-unit linkages and aliphatic end-units of the dimeric and trimeric
580 oligomers was revealed. The similar structural motifs (*i.e.* inter-unit linkages and end-units) of

581 these dimers and trimers disclose that they are subjected to the same chemical transformation
582 during the RCF process, a claim that can tentatively also be transferred to larger oligomers.
583 Accumulation of the GC × GC quantified products with regard to end groups and inter-linkages
584 agrees with recently acquired bulk ¹H-¹³C HSQC NMR spectroscopic information. This study
585 demonstrates a methodology using GC × GC in combination with recent ¹H-¹³C HSQC NMR
586 spectroscopic findings to advance the molecular structural information of RCF lignin. Thus, we
587 encourage future RCF lignin related research to implement such combined analysis as to
588 maximize their insights. Future GC x GC FID/MS dedicated research should focus on
589 identifying more dimers and trimers by analyzing mass spectra, possibly in combination with
590 NMR, organic synthesis, and purification strategies. Besides it might also be helpful to
591 characterize lignin repolymerization products, not only in RCF lignin oil but also in other lignin
592 types. Ultimately, the molecular information will enable the community to more rigorously
593 assess the chemical transformations that lignin undergoes during RCF biorefinery processing
594 as well as to steer further research in downstream lignin oil usage, functionalization and
595 separations, and corresponding application development.

596

597 **Acknowledgements**

598 The research leading to these results has received funding from the Catalisti-SBO Project
599 NIBCON. B.S, S. V. D. B., and K. V. A. also acknowledge funding through FWO-SBO project
600 BioWood and acknowledge that this project had received funding from the Bio-based Industries
601 Joint Undertaking under the European Union's Horizon 2020 research and innovation
602 programme under grant agreement No 837890 (SMARTBOX) and from the national EoS
603 (BIOFACT) and Flemish iBOF (NextBioRef) programs. S. V. D. B. acknowledges Flanders
604 Innovation & Entrepreneurship (Innovation Mandate). Furthermore, Kevin M. Van Geem is
605 holder of the ERC Grant OPTIMA (Process Intensification and Innovation in Olefin Production
606 by Multiscale Analysis and Design) with the grant agreement ID 818607. This work was
607 authored in part by the National Renewable Energy Laboratory, operated by the Alliance for
608 Sustainable Energy, LLC, for the U.S. Department of Energy (DOE) under Contract No. DE-
609 AC36-08GO28308. Funding was provided to RK and GTB by the U.S. DOE Office of Energy
610 Efficiency and Renewable Energy Bioenergy Technologies Office. The views expressed in the
611 article do not necessarily represent the views of the DOE or the U.S. Government. The U.S.
612 Government retains and the publisher, by accepting the article for publication, acknowledges
613 that the U.S. Government retains a nonexclusive, paid-up, irrevocable, worldwide license to

614 publish or reproduce the published form of this work, or allow others to do so, for U.S.
615 Government purposes.

616

617 **References**

618

619 1 A. J. Ragauskas, C. K. Williams, B. H. Davison, G. Britovsek, J. Cairney, C. A. Eckert,
620 W. J. Frederick, J. P. Hallett, D. J. Leak, C. L. Liotta, J. R. Mielenz, R. Murphy, R.
621 Templer and T. Tschaplinski, *Science*, 2006, **311**, 484–489.

622 2 A. J. Ragauskas, G. T. Beckham, M. J. Bidy, R. Chandra, F. Chen, M. F. Davis, B. H.
623 Davison, R. A. Dixon, P. Gilna, M. Keller, P. Langan, A. K. Naskar, J. N. Saddler, T.
624 J. Tschaplinski, G. A. Tuskan and C. E. Wyman, *Science*, ,
625 DOI:10.1126/science.1246843.

626 3 J. Ralph, C. Lapierre and W. Boerjan, *Current Opinion in Biotechnology*, 2019, **56**,
627 240–249.

628 4 W. Schutyser, T. Renders, S. Van Den Bosch, S. F. Koelewijn, G. T. Beckham and B.
629 F. Sels, *Chemical Society Reviews*, 2018, **47**, 852–908.

630 5 J. Zhang, Y. Jiang, L. F. Easterling, A. Anstner, W. Li, K. Z. Alzarieni, X. Dong, J.
631 Bozell and H. I. Kenttämä, *Green Chem.*, 2021, **23**, 983–1000.

632 6 C. Zhao, Z. Hu, L. Shi, C. Wang, F. Yue, S. Li, H. Zhang and F. Lu, *Green Chem.*,
633 2020, **22**, 7366–7375.

634 7 F. Yue, F. Lu, M. Regner, R. Sun and J. Ralph, *ChemSusChem*, 2017, **10**, 830–835.

635 8 A. De Santi, M. V Galkin, C. W. Lahive, P. J. Deuss and K. Barta, *ChemSusChem*,
636 2020, **13**, 4468.

637 9 A. Kumar and B. Thallada, *Sustainable Energy Fuels*, 2021, **5**, 3802–3817.

638 10 J. Zhu, C. Yan, X. Zhang, C. Yang, M. Jiang and X. Zhang, *Progress in Energy and*
639 *Combustion Science*, 2020, **76**, 100788.

640 11 X. Dou, W. Li, C. Zhu and X. Jiang, *Applied Catalysis B: Environmental*, 2021, **287**,
641 119975.

642 12 F. Wang, D. Ouyang, Z. Zhou, S. J. Page, D. Liu and X. Zhao, *Journal of Energy*
643 *Chemistry*, 2021, **57**, 247–280.

644 13 Y. Liao, S. F. Koelewijn, G. van den Bossche, J. van Aelst, S. van den Bosch, T.

645 Renders, K. Navare, T. Nicolai, K. van Aelst, M. Maesen, H. Matsushima, J. M.

646 Thevelein, K. van Acker, B. Lagrain, D. Verboekend and B. F. Sels, *Science*, 2020,

- 647 **367**, 1385–1390.
- 648 14 Y.-Y. Wang, C. E. Wyman, C. M. Cai and A. J. Ragauskas, *ACS Applied Polymer*
649 *Materials*, 2019, **1**, 1672–1679.
- 650 15 W. Zhang, Y. Ma, C. Wang, S. Li, M. Zhang and F. Chu, *Industrial Crops and*
651 *Products*, 2013, **43**, 326–333.
- 652 16 S. Nikafshar, J. Wang, K. Dunne, P. Sangthongantotai and M. Nejad, *ChemSusChem*,
653 2021, **14**, 1184–1195.
- 654 17 K. Van Aelst, E. Van Sinay, T. Vangeel, Y. Zhang, T. Renders, S. den Bosch, J. Van
655 Aelst and B. Sels, *Chem. Commun.*, 2021.
- 656 18 S. Van Den Bosch, W. Schutyser, R. Vanholme, T. Driessen, S. F. Koelewijn, T.
657 Renders, B. De Meester, W. J. J. Huijgen, W. Dehaen, C. M. Courtin, B. Lagrain, W.
658 Boerjan and B. F. Sels, *Energy and Environmental Science*, 2015, **8**, 1748–1763.
- 659 19 M. V Galkin, A. T. Smit, E. Subbotina, K. A. Artemenko, J. Bergquist, W. J. J.
660 Huijgen and J. S. M. Samec, *ChemSusChem*, 2016, **9**, 3280–3287.
- 661 20 E. M. Anderson, M. L. Stone, R. Katahira, M. Reed, G. T. Beckham and Y. Román-
662 Leshkov, *Joule*, 2017, **1**, 613–622.
- 663 21 T. Parsell, S. Yohe, J. Degenstein, T. Jarrell, I. Klein, E. Gencer, B. Hewetson, M.
664 Hurt, J. I. Kim, H. Choudhari, B. Saha, R. Meilan, N. Mosier, F. Ribeiro, W. N.
665 Delgass, C. Chapple, H. I. Kenttämä, R. Agrawal and M. M. Abu-Omar, *Green*
666 *Chem.*, 2015, **17**, 1492–1499.
- 667 22 P. Ferrini and R. Rinaldi, *Angewandte Chemie International Edition*, 2014, **53**, 8634–
668 8639.
- 669 23 Y. M. Questell-Santiago, M. V Galkin, K. Barta and J. S. Luterbacher, *Nature Reviews*
670 *Chemistry*, 2020, **4**, 311–330.
- 671 24 T. Renders, G. Van den Bossche, T. Vangeel, K. Van Aelst and B. Sels, *Current*
672 *Opinion in Biotechnology*, 2019, **56**, 193–201.
- 673 25 T. Renders, S. den Bosch, S.-F. Koelewijn, W. Schutyser and B. F. Sels, *Energy*
674 *Environ. Sci.*, 2017, **10**, 1551–1557.
- 675 26 T. Renders, S. Van Den Bosch, T. Vangeel, T. Ennaert, S. F. Koelewijn, G. Van Den
676 Bossche, C. M. Courtin, W. Schutyser and B. F. Sels, *ACS Sustainable Chemistry and*
677 *Engineering*, 2016, **4**, 6894–6904.
- 678 27 K. Van Aelst, E. Van Sinay, T. Vangeel, E. Cooreman, G. Van den Bossche, T.
679 Renders, J. Van Aelst, S. Van den Bosch and B. Sels, *Chemical Science*, ,
680 DOI:10.1039/d0sc04182c.

- 681 28 H. Li and G. Song, *ACS Catalysis*, 2019, **9**, 4054–4064.
- 682 29 Z. Sun, J. Cheng, D. Wang, T.-Q. Yuan, G. Song and K. Barta, *ChemSusChem*, 2020,
683 1–15.
- 684 30 M. M. Abu-Omar, K. Barta, G. T. Beckham, J. S. Luterbacher, J. Ralph, R. Rinaldi, Y.
685 Román-Leshkov, J. S. M. Samec, B. F. Sels and F. Wang, *Energy Environ. Sci.*, 2020,
686 **14**, 262–292.
- 687 31 Z. Sun, J. Cheng, D. Wang, T.-Q. Yuan, G. Song and K. Barta, *ChemSusChem*, ,
688 DOI:10.1002/cssc.202001085.
- 689 32 M. V Galkin and J. S. M. Samec, *ChemSusChem*, 2016, **9**, 1544–1558.
- 690 33 E. Cooreman, T. Vangeel, K. Van Aelst, J. Van Aelst, J. Lauwaert, J. W. Thybaut, S.
691 Van den Bosch and B. F. Sels, *Industrial & Engineering Chemistry Research*, 2020,
692 **59**, 17035–17045.
- 693 34 T. I. Korányi, B. Fridrich, A. Pineda and K. Barta, *Molecules*, ,
694 DOI:10.3390/molecules25122815.
- 695 35 C. Crestini, H. Lange, M. Sette and D. S. Argyropoulos, *Green Chem.*, 2017, **19**, 4104–
696 4121.
- 697 36 X. Jiang, D. Savithri, X. Du, S. Pawar, H. Jameel, H. Chang and X. Zhou, *ACS*
698 *Sustainable Chemistry & Engineering*, 2017, **5**, 835–842.
- 699 37 M. Gigli and C. Crestini, *Green Chem.*, 2020, **22**, 4722–4746.
- 700 38 R. Ebrahimi Majdar, A. Ghasemian, H. Resalati, A. Saraeian, C. Crestini and H. Lange,
701 *ACS Sustainable Chemistry & Engineering*, 2020, **8**, 16803–16813.
- 702 39 C. Allegretti, O. Boumezgane, L. Rossato, A. Strini, J. Troquet, S. Turri, G. Griffini
703 and P. D’Arrigo, *Molecules*, , DOI:10.3390/molecules25122893.
- 704 40 F. J. Calvo-Flores, G. G., Dobado, J.A., Isac-Garcia, J. and Martin-Martinez, *Lignin*
705 *and Lignans as renewable raw materials*, John Wiley & Sons, Ltd, 2015.
- 706 41 H. Lange, P. Gianni and C. Crestini, in *Lignin Valorization: Emerging Approaches*,
707 The Royal Society of Chemistry, 2018, pp. 413–476.
- 708 42 J. S. Lupoi, S. Singh, R. Parthasarathi, B. A. Simmons and R. J. Henry, *Renewable and*
709 *Sustainable Energy Reviews*, 2015, **49**, 871–906.
- 710 43 H. Ma, H. Li, W. Zhao, L. Li, S. Liu, J. Long and X. Li, *Green Chem.*, 2019, **21**, 658–
711 668.
- 712 44 C. S. Lancefield, S. Constant, P. de Peinder and P. C. A. Bruijninx, *ChemSusChem*,
713 2019, **12**, 1139–1146.
- 714 45 X. Bai, K. H. Kim, R. C. Brown, E. Dalluge, C. Hutchinson, Y. J. Lee and D. Dalluge,

- 715 *Fuel*, 2014, **128**, 170–179.
- 716 46 T. Renders, W. Schutyser, S. Van den Bosch, S.-F. Koelewijn, T. Vangeel, C. M.
717 Courtin and B. F. Sels, *ACS Catalysis*, 2016, **6**, 2055–2066.
- 718 47 Y. S. Choi, P. A. Johnston, R. C. Brown, B. H. Shanks and K.-H. Lee, *Journal of*
719 *Analytical and Applied Pyrolysis*, 2014, **110**, 147–154.
- 720 48 M. B. Figueirêdo, R. H. Venderbosch, H. J. Heeres and P. J. Deuss, *Journal of*
721 *Analytical and Applied Pyrolysis*, 2020, **149**, 104837.
- 722 49 M. D. M. Arruda, S. da Paz Leôncio Alves, I. J. da Cruz Filho, G. F. de Sousa, G. A. de
723 Souza Silva, D. K. D. do Nascimento Santos, M. do Carmo Alves de Lima, G. J. de
724 Moraes Rocha, I. A. de Souza and C. M. L. de Melo, *International Journal of*
725 *Biological Macromolecules*, 2021, **180**, 286–298.
- 726 50 F. Leng, Y. Wang, J. Chen, S. Wang, J. Zhou and Z. Luo, *Chinese Journal of Chemical*
727 *Engineering*, 2017, **25**, 324–329.
- 728 51 H. N. Lyckeskog, C. Mattsson, L. Olausson, S.-I. Andersson, L. Vamling and H.
729 Theliander, *Biomass Conversion and Biorefinery*, 2017, **7**, 401–414.
- 730 52 E. M. Anderson, M. L. Stone, R. Katahira, M. Reed, W. Muchero, K. J. Ramirez, G. T.
731 Beckham and Y. Román-Leshkov, *Nature Communications*, 2019, **10**, 2033.
- 732 53 D. C. Dayton and T. D. Foust, in *Emerging Issues in Analytical Chemistry*, eds. D. C.
733 Dayton and T. D. B. T.-A. M. for B. C. and C. Foust, Elsevier, 2020, pp. 75–88.
- 734 54 M. Kinne, M. Poraj-Kobielska, R. Ullrich, P. Nousiainen, J. Sipilä, K. Scheibner, K. E.
735 Hammel and M. Hofrichter, 2011, **65**, 673–679.
- 736 55 E. Kiyota, P. Mazzafera and A. C. H. F. Sawaya, *Analytical Chemistry*, 2012, **84**,
737 7015–7020.
- 738 56 B. C. Owen, L. J. Hauptert, T. M. Jarrell, C. L. Marcum, T. H. Parsell, M. M. Abu-
739 Omar, J. J. Bozell, S. K. Black and H. I. Kenttämäa, *Analytical Chemistry*, 2012, **84**,
740 6000–6007.
- 741 57 D. Tomasini, F. Cacciola, F. Rigano, D. Sciarrone, P. Donato, M. Beccaria, E. B.
742 Caramão, P. Dugo and L. Mondello, *Analytical Chemistry*, 2014, **86**, 11255–11262.
- 743 58 H. Sheng, W. Tang, J. Gao, J. S. Riedeman, G. Li, T. M. Jarrell, M. R. Hurt, L. Yang,
744 P. Murria, X. Ma, J. J. Nash and H. I. Kenttämäa, *Analytical Chemistry*, 2017, **89**,
745 13089–13096.
- 746 59 S. O. Asare, K. R. Dean and B. C. Lynn, *Analytical and Bioanalytical Chemistry*, 2021,
747 **413**, 4037–4048.
- 748 60 J. Zhang, Y. Jiang, A. Astner, H. Zhu, J. J. Bozell and H. I. Kenttämäa, *Green Chem.*,

- 749 2021, **23**, 4024–4033.
- 750 61 W. Schutyser, S. Van Den Bosch, T. Renders, T. De Boe, S.-F. F. Koelewijn, A.
751 Dewaele, T. Ennaert, O. Verkinderen, B. Goderis, C. M. Courtin and B. F. Sels, *Green*
752 *Chemistry*, 2015, **17**, 5035–5045.
- 753 62 S. Van Den Bosch, W. Schutyser, S.-F. F. Koelewijn, T. Renders, C. M. Courtin and B.
754 F. Sels, *Chemical Communications*, 2015, **51**, 13158–13161.
- 755 63 Y. Wang, R. Yin, M. Chai, Nishu, C. Li, M. Sarker and Ronghou Liu, *Journal of the*
756 *Energy Institute*, 2020, **93**, 2163–2175.
- 757 64 Z. Ji-lu, *Journal of Analytical and Applied Pyrolysis*, 2007, **80**, 30–35.
- 758 65 K. G. Kalogiannis, S. D. Stefanidis, C. M. Michailof, A. A. Lappas and E. Sjöholm,
759 *Journal of Analytical and Applied Pyrolysis*, 2015, **115**, 410–418.
- 760 66 M. R. Djokic, T. Dijkmans, G. Yildiz, W. Prins and K. M. Van Geem, *Journal of*
761 *Chromatography A*, 2012, **1257**, 131–140.
- 762 67 C. Michailof, T. Sfetsas, S. Stefanidis, K. Kalogiannis, G. Theodoridis and A. Lappas,
763 *Journal of Chromatography A*, 2014, **1369**, 147–160.
- 764 68 T. Sfetsas, C. Michailof, A. Lappas, Q. Li and B. Kneale, *Journal of Chromatography*
765 *A*, 2011, **1218**, 3317–3325.
- 766 69 F. Mao, H. Fan and J. Wang, *Journal of Analytical and Applied Pyrolysis*, 2019, **139**,
767 213–223.
- 768 70 N. V. Hung, C. Mohabeer, M. Vaccaro, S. Marcotte, V. Agasse-Peulon, L.
769 Abdelouahed, B. Taouk and P. Cardinael, *Journal of Mass Spectrometry*, 2020, **55**,
770 e4495.
- 771 71 V. O. Nunes, R. V. S. Silva, G. A. Romeiro and D. A. Azevedo, *Microchemical*
772 *Journal*, 2020, **153**, 104514.
- 773 72 R. V. S. Silva, N. S. Tessarolo, V. B. Pereira, V. L. Ximenes, F. L. Mendes, M. B. B.
774 de Almeida and D. A. Azevedo, *Talanta*, 2017, **164**, 626–635.
- 775 73 C. R. Kumar, N. Anand, A. Kloekhorst, C. Cannilla, G. Bonura, F. Frusteri, K. Barta
776 and H. J. Heeres, *Green Chem.*, 2015, **17**, 4921–4930.
- 777 74 L. Negahdar, A. Gonzalez-Quiroga, D. Otyuskaya, H. E. Toraman, L. Liu, J. T. B. H.
778 Jastrzebski, K. M. Van Geem, G. B. Marin, J. W. Thybaut and B. M. Weckhuysen,
779 *ACS Sustainable Chemistry & Engineering*, 2016, **4**, 4974–4985.
- 780 75 C. M. Michailof, K. G. Kalogiannis, T. Sfetsas, D. T. Patiaka and A. A. Lappas, *WIREs*
781 *Energy and Environment*, 2016, **5**, 614–639.
- 782 76 R. Vendamme, J. Behaghel de Bueren, J. Gracia-Vitoria, F. Isnard, M. M. Mulunda, P.

- 783 Ortiz, M. Wadekar, K. Vanbroekhoven, C. Wegmann, R. Buser, F. Héroguel, J. S.
784 Luterbacher and W. Eevers, *Biomacromolecules*, 2020, *acs.biomac.0c00927*.
- 785 77 J. E. Q. Quinsaat, E. Feghali, D. J. van de Pas, R. Vendamme and K. M. Torr, *ACS*
786 *Applied Polymer Materials*, 2021, **3**, 5845–5856.
- 787 78 E. Feghali, D. J. van de Pas and K. M. Torr, *Biomacromolecules*, 2020, **21**, 1548–1559.
- 788 79 J. S. Mahajan, R. M. O’Dea, J. B. Norris, L. T. J. Korley and T. H. Epps, *ACS*
789 *Sustainable Chemistry & Engineering*, 2020, **8**, 15072–15096.
- 790 80 A. Moreno and M. H. Sipponen, *Mater. Horiz.*, 2020, **7**, 2237–2257.
- 791 81 M. N. Collins, M. Nechifor, F. Tanasă, M. Zănoagă, A. McLoughlin, M. A. Strózyk,
792 M. Culebras and C.-A. Teacă, *International Journal of Biological Macromolecules*,
793 2019, **131**, 828–849.
- 794 82 I. Zaborniak, P. Chmielarz and K. Matyjaszewski, *European Polymer Journal*, 2019,
795 **120**, 109253.
- 796 83 M. A. Jedrzejczyk, S. Van den Bosch, J. Van Aelst, K. Van Aelst, P. D. Kouris, M.
797 Moalin, G. R. M. M. Haenen, M. D. Boot, E. J. M. Hensen, B. Lagrain, B. F. Sels and
798 K. V. Bernaerts, *ACS Sustainable Chemistry & Engineering*, 2021, **9**, 12548–12559.
- 799 84 E. O. Ebikade, N. Samulewicz, S. Xuan, J. D. Sheehan, C. Wu and D. G. Vlachos,
800 *Green Chem.*, 2020, **22**, 7435–7447.
- 801 85 A. Parodi, E. Diguilio, S. Renzini and I. Magario, *Carbohydrate Research*, 2020, **487**,
802 107885.
- 803 86 J.-Y. de Saint Laumer, S. Leocata, E. Tissot, L. Baroux, D. M. Kampf, P. Merle, A.
804 Boschung, M. Seyfried and A. Chaintreau, *Journal of Separation Science*, 2015, **38**,
805 3209–3217.
- 806 87 J.-Y. de Saint Laumer, E. Cicchetti, P. Merle, J. Egger and A. Chaintreau, *Analytical*
807 *Chemistry*, 2010, **82**, 6457–6462.
- 808 88 S. Y. Park, J.-Y. Kim, H. J. Youn and J. W. Choi, *International Journal of Biological*
809 *Macromolecules*, 2018, **106**, 793–802.
- 810 89 C. S. Lancefield, H. L. J. Wienk, R. Boelens, B. M. Weckhuysen and P. C. A.
811 Bruijninx, *Chem. Sci.*, 2018, **9**, 6348–6360.
- 812 90 R. Rinaldi, R. Jastrzebski, M. T. Clough, J. Ralph, M. Kennema, P. C. A. A. Bruijninx
813 and B. M. Weckhuysen, *Angewandte Chemie - International Edition*, 2016, **55**, 8164–
814 8215.
- 815 91 H. Li and G. Song, *ACS Catalysis*, , DOI:10.1021/acscatal.0c02339.
- 816 92 F. Yue, F. Lu, S. Ralph and J. Ralph, *Biomacromolecules*, 2016, **17**, 1909–1920.

817 93 Y. Li, T. Akiyama, T. Yokoyama and Y. Matsumoto, *Biomacromolecules*, 2016, **17**,
818 1921–1929.
819
820